



Contrasting Effects of Local Environmental and Biogeographic Factors on the Composition and Structure of Bacterial Communities in Arid Monospecific Mangrove Soils

 T. Thomson,^{a,b}  M. Fusi,^{b,c}  M. F. Bennett-Smith,^b  N. Prinz,^a  E. Aylagas,^b  S. Carvalho,^b  C. E. Lovelock,^d  B. H. Jones,^b
 J. I. Ellis^{a,b}

^aUniversity of Waikato, School of Science, Tauranga, New Zealand

^bKing Abdullah University of Science and Technology (KAUST), Biological and Environmental Sciences and Engineering Division (BESE), Thuwal, Saudi Arabia

^cSchool of Applied Sciences, Edinburgh Napier University, Edinburgh, United Kingdom

^dSchool of Biological Sciences, The University of Queensland, St Lucia, Australia

ABSTRACT Mangrove forests are important biotic sinks of atmospheric CO₂ and play an integral role in nutrient-cycling and decontamination of coastal waters, thereby mitigating climatic and anthropogenic stressors. These services are primarily regulated by the activity of the soil microbiome. To understand how environmental changes may affect this vital part of the ecosystem, it is key to understand the patterns that drive microbial community assembly in mangrove forest soils. High-throughput amplicon sequencing (16S rRNA) was applied on samples from arid *Avicennia marina* forests across different spatial scales from local to regional. Alongside conventional analyses of community ecology, microbial co-occurrence networks were assessed to investigate differences in composition and structure of the bacterial community. The bacterial community composition varied more strongly along an intertidal gradient within each mangrove forest, than between forests in different geographic regions (Australia/Saudi Arabia). In contrast, co-occurrence networks differed primarily between geographic regions, illustrating that the structure of the bacterial community is not necessarily linked to its composition. The local diversity in mangrove forest soils may have important implications for the quantification of biogeochemical processes and is important to consider when planning restoration activities.

IMPORTANCE Mangrove ecosystems are increasingly being recognized for their potential to sequester atmospheric carbon, thereby mitigating the effects of anthropogenically driven greenhouse gas emissions. The bacterial community in the soils plays an important role in the breakdown and recycling of carbon and other nutrients. To assess and predict changes in carbon storage, it is important to understand how the bacterial community is shaped by its environment. Here, we compared the bacterial communities of mangrove forests on different spatial scales, from local within-forest to biogeographic comparisons. The bacterial community composition differed more between distinct intertidal zones of the same forest than between forests in distant geographic regions. The calculated network structure of theoretically interacting bacteria, however, differed most between the geographic regions. Our findings highlight the importance of local environmental factors in shaping the microbial soil community in mangroves and highlight a disconnect between community composition and structure in microbial soil assemblages.

KEYWORDS microbiome, 16S rRNA, microbial biogeography, ecological processes, community structure, co-occurrence network analysis, community assembly

Mangrove forests are among the world's most efficient natural "Blue Carbon" sinks (1). About three-quarters (76.5%) of the carbon bound in mangrove forests is stored in the soil (1, 2). This globally important ecosystem service is mainly driven by

Editor Allison Veach, University of Texas at San Antonio

Copyright © 2022 Thomson et al. This is an open-access article distributed under the terms of the [Creative Commons Attribution 4.0 International license](https://creativecommons.org/licenses/by/4.0/).

Address correspondence to T. Thomson, timi.thomson@gmail.com.

The authors declare no conflict of interest.

Received 13 July 2021

Accepted 11 December 2021

Published 5 January 2022

the activity of the associated soil microbial communities (3–6). In particular, mangrove soil bacteria comprise up to 30% of the soil biomass and play a pivotal role in regulating the forest's biochemical processes (7, 8). Yet, despite their role in carbon sequestration and additional ecosystem services microbial communities have not received the same attention as those in other environments such as coral reefs, the pelagic ocean, forests, and agricultural pastures (9–12).

Mangrove soils are characterized by high spatial heterogeneity of their physical, chemical, and biological components (13). Notably, leaf and root litter are hot spots of microbial activity due to decomposition (14–16). Oxygen is usually confined to the uppermost millimeters of the soil profile, but the presence of aerial roots and burrowing organisms can introduce oxygen into deeper layers (17–19). Such settings create microhabitats that support a wide range of microbial assemblages (20). On a wider spatial scale, mangrove forests display a distinct zonation between the seaward edge where tall fringing forests occur, and the interior of the forest where shrub forms of mangrove often dominate (21). Tree height, nutrient availability, productivity, bioturbation, salinity, and hydrology create contrasting settings between these zones, greatly influencing the physicochemical parameters of the soil (13, 17, 22–25). Studies on small-scale distributions (centimetres to meters) of microbial communities along environmental gradients (e.g., bioturbated soil by animal burrowing or plant root growth) have identified high levels of community variability, thereby confirming the complex patchwork of microbial assemblages in mangrove soils (19, 26–28). Despite this high intraforest variation, comparisons of microbial communities of mangrove soils between forests (on regional and global scales) yielded high levels of similarity (29–31). This emphasizes the importance of the local environmental conditions in determining the soil microbiome which have received increased attention recently (32–35). However, there is still limited research on the variation of these factors on a larger scale and little is known about the factors that influence bacterial community assembly in mangrove soils (36).

In community ecology, the nature and mechanisms of species distributions are widely studied and have largely been adapted by the field of microbial ecology (37, 38). It is now widely agreed that microorganisms follow biogeographic patterns similar to those of macroorganisms, and are limited by a combination of historical and geographic/environmental settings (37–41). This framework of community assembly recognizes four key processes that shape ecological communities that can be of stochastic or deterministic nature: selection, drift, speciation, and dispersal (37). Extrinsic processes on various spatial scales that are associated with species pools and dispersion influence community composition as do intrinsic environmental and biotic processes (42). As soil microbial communities of mangrove forests facilitate ecosystem processes of global importance, understanding the mechanisms that shape microbial community composition can aid in predicting changes resulting from fluctuating environmental and climatic conditions (12, 39). While there have been recent efforts to better understand microbial community assembly in both coastal and mangrove sediments (36, 43), a novel aspect of this study is the use of a hierarchical study design that takes into account various spatial scales.

Recent work indicates that, in order to ensure the functioning of an ecosystem, the structure of its microbial community is as important as its composition (44–47). Throughout this paper, we refer to community structure as network topology characteristics that imply interactions within the community, and we define community composition as alpha and beta diversity.

Network analyses of co-occurring microbial taxa have proven useful in the characterization of microbial community structures, despite the limitations of this statistical method, providing a solid sampling design and sufficient replication is considered (46, 48, 49). Disentangling patterns of connectedness between members of the microbial community and their spatial variability is an important step toward understanding the importance of single members or groups of the microbial community in facilitating

functional diversity and resilience (50). The functional diversity of a system describes the traits of organisms present within it that potentially influence or contribute to changes in this system (51). Ecological and functional microbial redundancies are key drivers of ecosystem resilience (49). As mangroves are threatened by numerous factors (e.g., sea level rise, overexploitation, drought, increased/decreased salinity) (52–54), patterns of microbial biodiversity can provide insights on the effective capacity of the mangrove to buffer these changes.

Based on the evidence above, we hypothesized that local environmental parameters are important controlling factors of the soil bacterial community, which may exceed the importance of geographic region. Therefore, we expected soil bacterial communities associated with the same species of mangroves and under similar climate conditions to vary more on local scales compared to variation at global scales. Moreover, physico-chemical conditions in different forests and between forest zones will have a significant influence on soil bacterial networks and the keystone taxa within them.

To test our hypotheses, we compared the bacterial community of two monospecific *Avicennia marina* mangrove forests over various spatial scales using 16S rRNA gene sequencing, aiming to identify the selective forces that determine the bacterial assembly patterns within the microbiome in this highly specialized environment. We analyzed the bacterial communities at different depths in the soil, distance from the sea, in forests with different exposures to oceanic influences, and from two distant geographic regions that are both dominated by a hot and arid climate (i.e., Saudi Arabia and Australia) (55).

RESULTS

Diversity of bacterial communities. The rank-abundance relationship displayed in Fig. 1A shows the disproportional abundance of rare amplicon sequence variants (ASVs) (high rank values) compared to few highly abundant ASVs in the community, which is consistent across all sampling sites. Notably, the subsurface samples from the shrub zone show the steepest decline along the ranks, indicating fewer highly prevalent ASVs in these samples. Other than that, no definite trends are obvious between the samples.

The species richness differed significantly for each combination of geographic region, exposure, and zone but not for depth (geographic region \times exposure \times zone; $F_{1,103} = 8.83$, P value = 0.004; Fig. 1B, Table S3). Species richness (observed ASVs) generally showed a significantly higher number of ASVs in Saudi Arabia compared to Australia (TukeyHSD, $P = 0.002$; 16.4% increase). In Australia, species richness was similar between the zones of the exposed site, while it varied significantly between zones of the sheltered site (TukeyHSD, $P = < 0.001$; 121.7% higher in the fringe) where the richness was higher in the soils of the tall fringing forest. In Saudi Arabia, species richness was generally higher in the shrub than in the fringe (TukeyHSD, $P = 0.02$; 17.4% increase).

The variation of the Shannon diversity index was only significant between the interaction of local factors (zone \times depth; $F_{1,104} = 5.28$, P value 0.02; Table S4). Except for the exposed site in Australia, the differences between depths in the soil were significant in the shrub zone of the forest (TukeyHSD, $P < 0.001$; 8.9% higher in the surface), with higher diversity scores in the surface layers of the soil (Fig. 1C).

The differences in phylogenetic diversity were significant between the factors geographic region, exposure, and zone (geographic region \times exposure \times zone; $F_{1,103} = 14.66$, P value < 0.001 ; Table S5). Phylogenetic diversity was highest in the shrub of Saudi Arabia and generally showed higher values for the shrub zone compared to the fringe (TukeyHSD, $P < 0.001$; 25.1% increase) (Fig. 1D). As with the Species richness and the Shannon diversity index, the phylogenetic diversity of the sheltered site in Australia showed an opposing trend between the zones, yielding higher diversity in the fringe compared to the shrub.

Composition of bacterial communities. The proportion (throughout the document referred to as relative abundances) of phyla between factors are shown in Fig. 2A and Table S6. *Proteobacteria* was the most abundant phylum across all samples

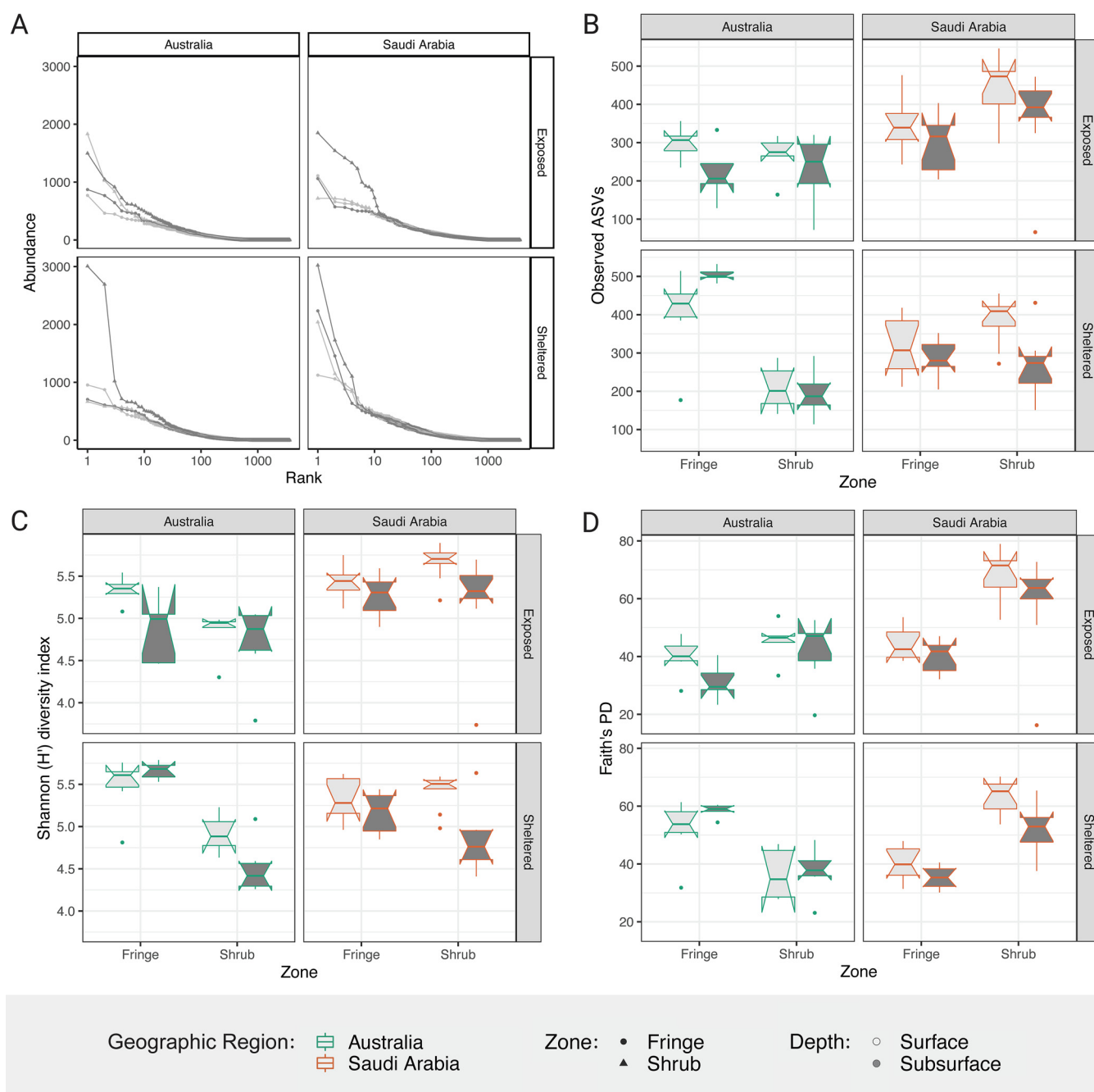


FIG 1 Within sample diversity of bacterial communities from arid mangrove soils. Alpha diversity measures of the bacterial communities detected in mangrove soils from Australia (green outline) and Saudi Arabia (orange outline) across zones (fringe, shrub) and depths (surface in light gray, subsurface in dark gray). (A) Rank-abundance relationship of ASVs by location. (B) Species richness described by the number of observed ASVs. (C) Shannon diversity index. (D) Phylogenetic diversity index (Faith's PD). The boxplots indicate the median with the interquartile range (IQR) between the 25th and the 75th percentile and the whiskers extend $1.5 \times \text{IQR}$. Boxes were plotted with the notch ($\pm 1.58 \times \text{IQR} / \sqrt{n}$) to display likely statistical significance if notches do not overlap.

(58.96%), followed by *Bacteroidetes* (17.44%), *Chloroflexi* (8.06%), *Calditrichaeota* (3.81%), and *Nitrospirae* (1.59%), contributing to 90% of the total community. Within *Proteobacteria*, the most abundant class was *Deltaproteobacteria* (31.60%), followed by *Gammaproteobacteria* (23.34%), *Bacteroidia* (13.65%), *Anaerolineae* (7.12%), and *Alphaproteobacteria* (4.44%) (Table S7). In the shrub zone, the differences in relative abundance of phyla between surface and subsurface was more obvious than in the tall fringing zone. This is consistent for exposed and sheltered sites in both geographic regions. Especially in the shrub samples, the relative abundances of *Proteobacteria* was

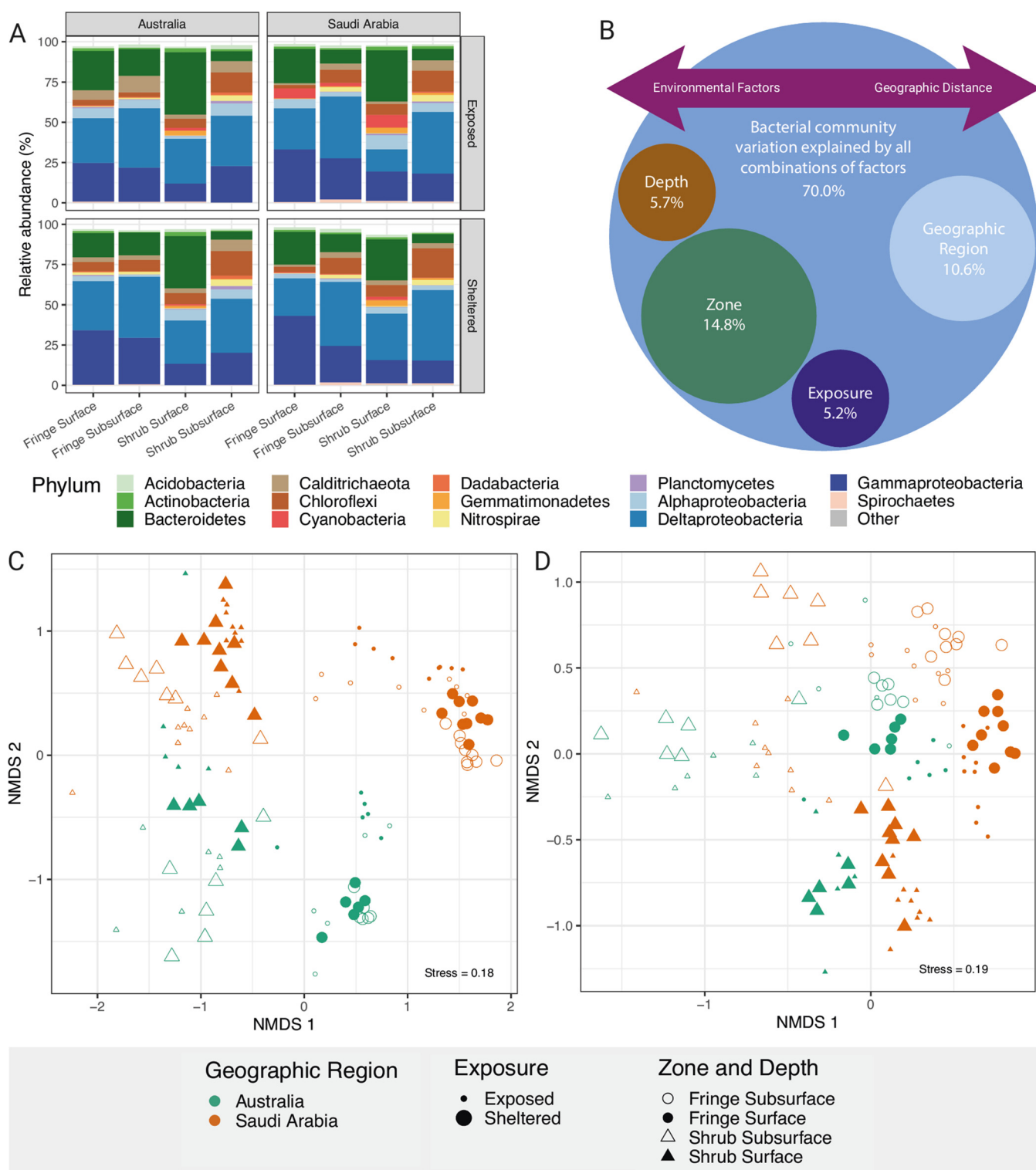


FIG 2 Comparison of different bacterial communities between the experimental factors geographic region, exposure, zone, and depth. (A) Relative abundance of phyla across the whole data set. The top 12 most prevalent phyla were displayed and the remaining grouped as "Other." The most abundant classes within the *Proteobacteria* were additionally included (blue colors). (B) Schematic representation of the R²-values from the PERMANOVA. The large bubble represents the proportion of variation explained by the interaction of all experimental factors. The small bubbles show the proportion of variation explained by each individual factor. The arrow above indicates the environmental factors influencing the separation. (C) Nonmetric multidimensional scaling (NMDS) plots of the community matrix across experimental factors at ASV level, and (D) at genus level across geographic region, exposure, zone and depth.

higher in the subsurface layer than at the surface (Fig. S3). *Deltaproteobacteria* were more abundant in the subsurface of all samples, while *Gammaproteobacteria* were generally more abundant in the fringing zone (Fig. 2A). The second most abundant phylum, *Bacteroidetes*, was more abundant in the surface layer of all locations (Fig. S4). *Chloroflexi*, *Calditrichaeota*, and *Nitrospirae* were more abundant in the subsurface layer, except from the fringe samples of the sheltered site in Australia (Fig. S5 to S7). *Cyanobacteria* were abundant at the surface and more so in Saudi Arabian samples. The relative abundances of *Cyanobacteria* were particularly high in both zones of the exposed site in Saudi Arabia with the exposed shrub of Australian samples also showing slightly elevated abundances (Fig. S8).

The NMDS plot (Stress = 0.18), calculated from the community matrix at ASV level, separates the samples by the factor zone along the first axis (Fig. 2C). The factor geographic region mainly accounts for the spread of the data points along the second axis. This is more obvious for the fringe samples, whereas the samples from the shrub overlap slightly, leading to a slight overlap of communities from different geographic regions. The factors exposure and depth fail to separate the samples into distinguishable groups. At genus level (Stress = 0.19), the factor zone still separated the samples; however, the factor geographic region did not (Fig. 2D). Instead, the factor depth was able to help separate the data in the ordination space, while the factor exposure did not. The models calculated from the CAP analysis were able to match the bacterial communities with the correct factor combination between 80 – 100% of the time at ASV level and genus level (13 and 11 perfect scores out of 16, respectively). The model at phylum level performed poorly (between 44.4 – 100%), which is why no further analysis was carried out at a higher taxonomic level.

PERMANOVA showed a significant interaction on the taxonomic community composition at ASV level across all factors (geographic region \times exposure \times zone \times depth; $F_{1,114} = 3.36$; P value = 0.001; Table S8). A pairwise comparison of the significant four-way interaction term confirmed the statistical significance between ecologically relevant combinations of the factors geographic region, exposure, zone, and depth (Table S9). A significant interaction term between geographic region, exposure, zone, and depth was found at genus level (geographic region \times exposure \times zone \times depth; $F_{1,114} = 3.99$; P value 0.002; Table S10). The variation within the data set explained by the individual factors was 10.6% by geographic region, 5.2% by exposure, 14.8% by zone, and 5.7% by depth (Table S8). All combinations of factors were able to constrain 70.0% of variation within the data set (Table S8).

Network analysis. The network analysis revealed distinct co-occurrence patterns between bacterial ASVs of mangrove soils across the factors of this study. The Australian networks contained a lower average number of nodes and a higher number of edges than Saudi Arabia, resulting in a higher density and average number of neighbors, but lower network diameter. The modularity, as indicated by the number of modules detected in each network, was higher in Saudi Arabia, whereas the clustering coefficient and the centralization was higher in Australian networks (Table 1, File S2).

The betweenness centrality metric per phylum showed differences between the experimental factors (Fig. 3A). The betweenness scores in Saudi Arabia seemed generally to be more evenly distributed between phyla than in Australia. This was driven by the high variability of *Calditrichaeota*, *Planctomycetes*, and *Spirochaetes* in Australian samples. Between zones, *Cyanobacteria* and *Zixibacteria* showed distinct differences. *Cyanobacteria* were more central in shrub samples of both geographic regions and *Zixibacteria* were also more central in the shrub samples. Between depths, *Cyanobacteria* and *Nitrospirae* varied. Values for *Cyanobacteria* were higher in the surface layers and *Nitrospirae* were more central in the subsurface of most samples. *Actinobacteria*, *Gemmatimonadetes*, and *Chloroflexi* showed consistently high betweenness centrality values, while values for *Proteobacteria* and *Bacteroidetes* were constant but average in all samples.

The topological coefficient highlighted the role of yet different phyla within the networks (Fig. 3B). As for the betweenness centrality, the values for the topological coefficient

TABLE 1 Summary statistics characterizing the bacterial co-occurrence networks of all sites in Australia and in Saudi Arabia

Geographic region	Exposure	Zone	Depth	Nodes	Edges	Edges per node	Clustering coefficient	Centralization	Diameter	Avg neighbors	Density	No. of modules
Australia	Exposed	Fringe	Surface	609	14793	24.29	0.58	0.52	7	48.58	0.08	6
			Subsurface	609	14793	24.29	0.58	0.52	7	48.58	0.08	6
		Shrub	Surface	451	6504	14.42	0.70	0.11	9	28.84	0.06	14
			Subsurface	597	8333	13.96	0.70	0.60	7	27.92	0.05	5
	Sheltered	Fringe	Surface	495	5808	11.73	0.62	0.67	6	23.47	0.05	5
			Subsurface	733	6323	8.63	0.44	0.40	7	17.25	0.02	6
		Shrub	Surface	675	2024	3.00	0.45	0.02	21	6.00	0.01	17
			Subsurface	418	5530	13.23	0.55	0.36	6	26.46	0.06	3
Saudi Arabia	Exposed	Fringe	Surface	423	9642	22.79	0.52	0.45	7	45.59	0.11	3
			Subsurface	736	5387	7.32	0.33	0.16	10	14.64	0.02	10
		Shrub	Surface	737	6088	8.26	0.37	0.26	7	16.52	0.02	10
			Subsurface	769	5514	7.17	0.37	0.29	8	14.34	0.02	8
	Sheltered	Fringe	Surface	726	5569	7.67	0.32	0.43	10	15.34	0.02	7
			Subsurface	661	4178	6.32	0.42	0.24	11	12.64	0.02	9
		Shrub	Surface	609	4812	7.90	0.38	0.22	8	15.80	0.03	7
			Subsurface	736	5725	7.78	0.30	0.31	11	15.56	0.02	9

were more evenly distributed between phyla in Saudi Arabian samples. Highly variable in Australian samples were *Actinobacteria* and *Cyanobacteria*. *Gemmatimonetes* showed high values in the soils of sheltered sites of Australian forests. Across zones, *Spirochaetes* and *Zixibacteria* showed the strongest differences with generally higher scores in the fringe. Between depths, *Spirochaetes* showed the greatest differences with generally slightly higher values in the Surface. Overall, *Nitrospirae*, *Spirochaetes*, *Zixibacteria*, and in some samples *Gemmatimonetes* had the highest scores. Keystone taxa analysis showed an increased number of important nodes in Saudi Arabian compared to Australian networks (Fig. S9).

In Australian networks, the relative proportion of nodes at higher degrees

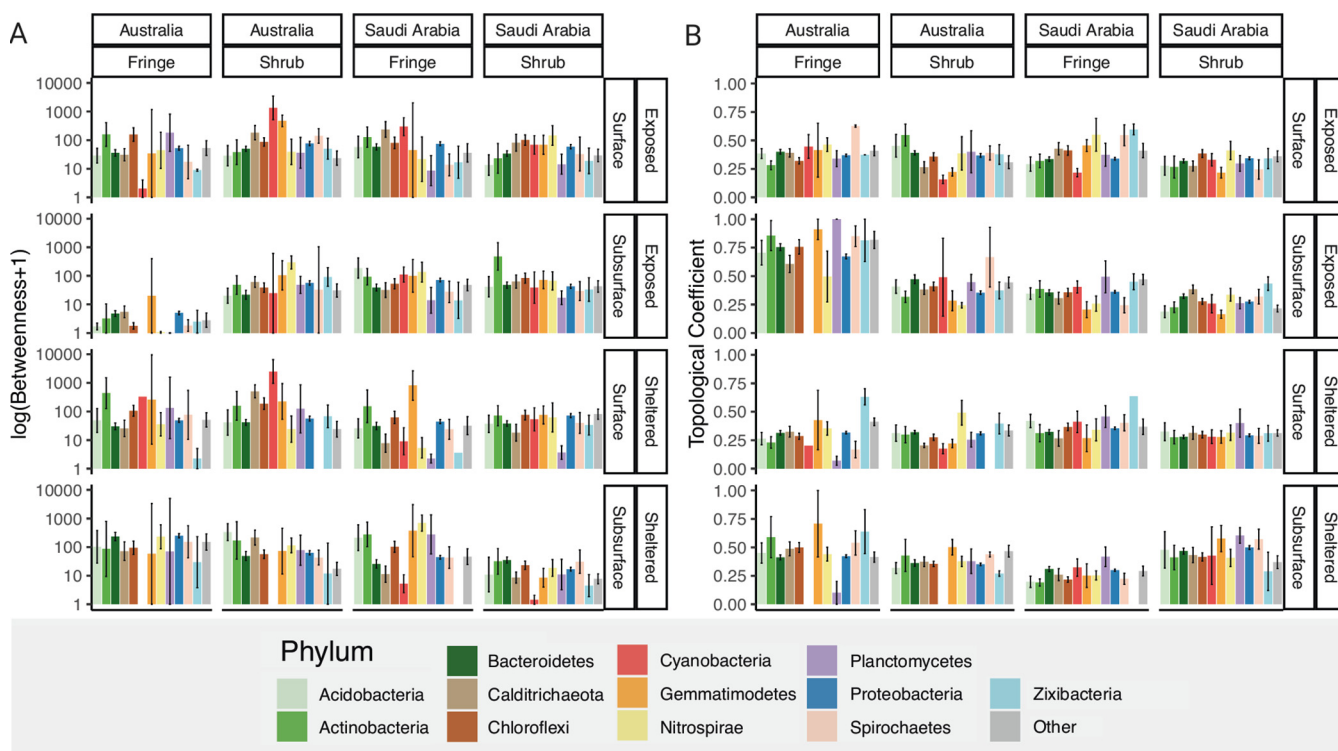


FIG 3 Selected network metrics by phylum. (A) Betweenness centrality and (B) Topological coefficient. The 12 most prevalent phyla (within the networks) were selected and the remaining grouped as "Other". Mean scores are displayed with standard errors calculated by the `stat_summary` function in `ggplot2`. Bars without standard errors display single occurrences.

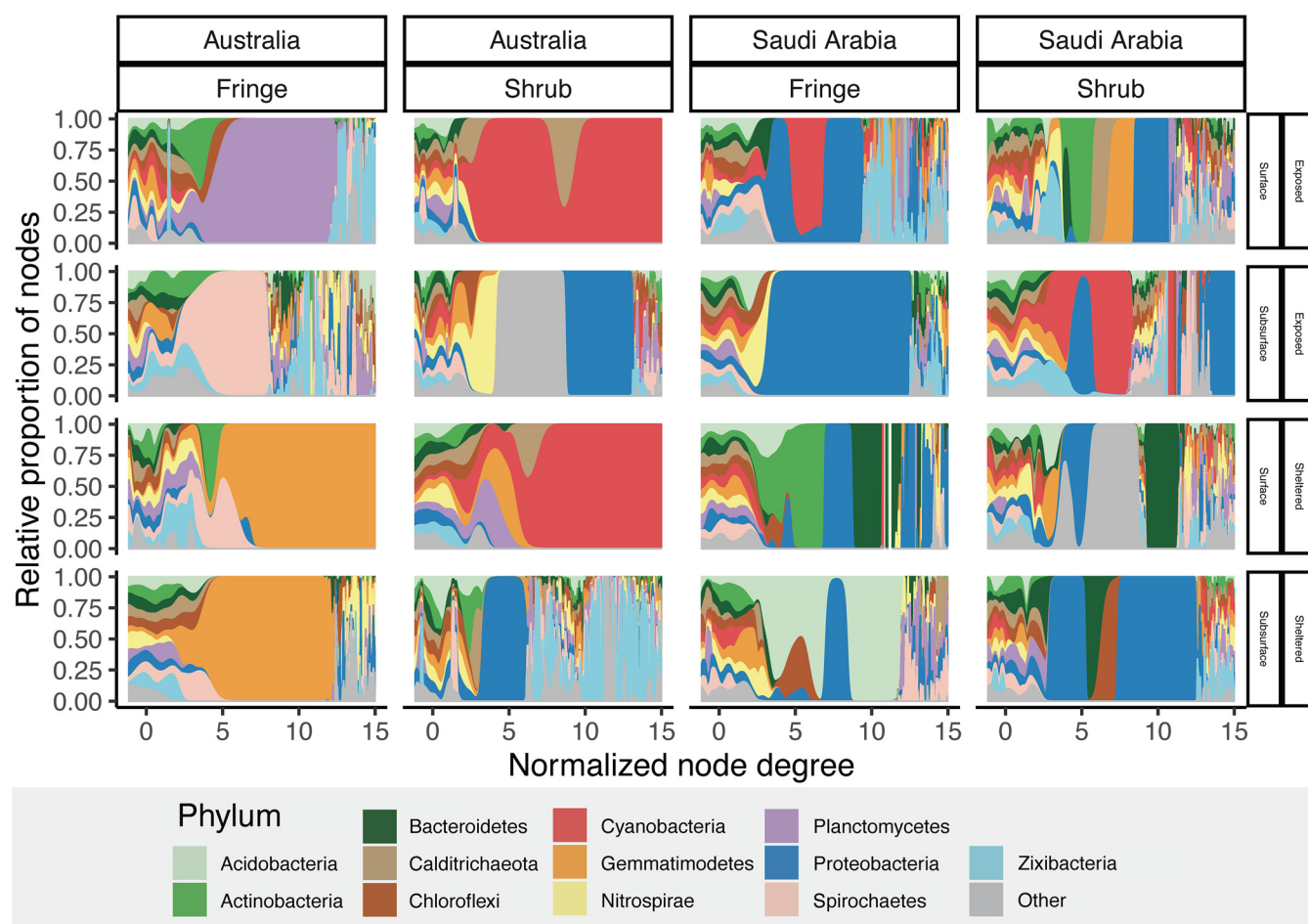


FIG 4 Comparison of high degree scores in co-occurrence networks. Density plots of the relative proportion of nodes against the normalized node degree colored by phylum across geographic region, exposure, zone and depth. The proportion of nodes is calculated by the Kernel-Density function.

(normalized) was dominated by single phyla, especially in the shrub forests (Fig. 4). In the surface samples of the shrub in Australia, *Cyanobacteria*, and at a lower node-degree *Calditrichaeota*, were the only phylum with normalized node-degrees higher than 5, whereas in the subsurface of the same samples *Proteobacteria*, *Zixibacteria*, and less abundant phyla (grouped as “Other”) filled this role. In the surface samples of the fringe in Australia, *Planctomycetes*, *Chloroflexi*, and *Actinobacteria* were most connected in exposed forests, and *Gemmatimonadetes* in the sheltered forests. This stands in a strong contrast to the Saudi Arabian sites, in which nodes with high degrees were shared between different phyla, thereby representing a higher diversity of highly connected nodes.

Functional assignments. Across all factors, “respiration of sulfur compounds” was the most prominent function, with an increased presence in the subsurface layer (Fig. 5). “Chemoheterotrophy” was an abundant pathway with higher prevalence in the surface layer, especially at the sheltered site in Saudi Arabia. Functional traits related to photosynthesis, such as “cyanobacteria” (grouped as a function by FAPROTAX), “phototrophy,” “photoautotrophy,” and “oxygenic photoautotrophy” were more abundant at the surface layers, most notably in the exposed site in Saudi Arabia. Generally, these functions were more abundant in the exposed site compared to the sheltered site. “Fermentation” was a prominent function in the sheltered site in Saudi Arabia, as well as the fringe samples of the other sites. “Aerobic nitrite oxidation” and “nitrification” were more abundant in the subsurface compared to the surface. The variation between all factors were statistically significant (geographic region \times exposure \times zone \times depth; PERMANOVA;

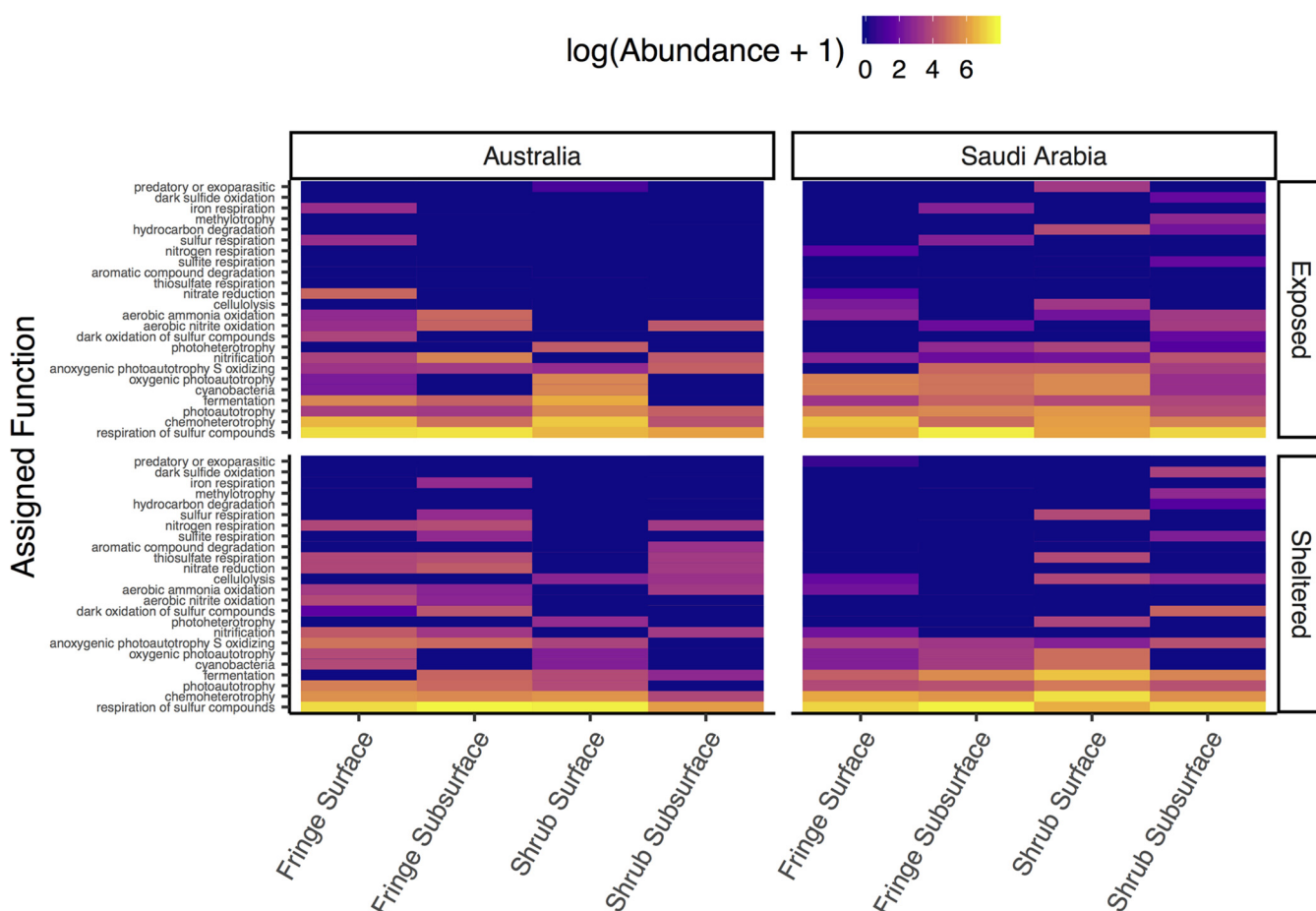


FIG 5 Theoretical functional assignments. Heat map showing the distributions of bacterial functions that were assigned by FAPROTAX across geographic region, exposure, zone and depth. Values were log-transformed with lighter values indicating higher abundances.

permutations = 999, method = bray, $F_{1,114} = 5.79$; P value = 0.001; Table S11), underlining the variability of the inferred function across factors.

DISCUSSION

Environmental factors characterizing distinct areas within arid *Avicennia marina* mangrove forests were more important in shaping the bacterial soil community than the geographic region of the forest based on community composition analysis. We found that the bacterial communities of mangrove soils differed significantly between geographic regions and local factors based on alpha- and beta-diversity. Furthermore, they were compositionally less similar between contrasting zones within a forest, than between different forests on a continental scale. In contrast, the hypothetical interaction structure of mangrove soil bacteria, as represented by co-occurrence networks, was strongly associated with the geographic region. This finding highlights potentially important differences between the composition and the co-occurrence structure of the microbial community. Consequently, the role of local environmental, and global factors is discussed in turn.

Local factors: the role of environmental variability. Mangrove forests are spatially heterogeneous along distinct intertidal and depth gradients within which the physicochemical conditions can differ dramatically (25, 56). In several studies on terrestrial and coastal soil microbiomes across different latitudes and ecosystems, environmental parameters (especially pH) were more influential on the community composition than geographic distance (11, 36, 43, 57). Similarly, a continuity of the microbial community driven by environmental factors has also been proposed for the pelagic

ocean, as well as for brackish water bodies (58, 59). Our results confirm a separation of the bacterial community following the structure of the forest, as has been suggested previously (60). The increased potential of dispersal at the fringe by freely moving water masses and the increased cycle of surface particle sedimentation and resuspension may lead to a homogenization of the bacterial communities in this zone (61, 62). The importance of tidal mixing for homogeneity of microbial communities is consistent with an earlier study that found the microbial soil community at the fringe of a mangrove soil to be more similar to that of the adjacent mudflat, than to the interior of the same forest (63). The number of observed ASVs increased significantly in the shrub of Saudi Arabian forests, as did the phylogenetic diversity, thus supporting the hypothesis of higher diversity away from the homogenizing forces of the fringe environment (64–66). In Australia these differences were less pronounced in the exposed site but opposite in the sheltered site with higher numbers of observed ASVs in the fringe compared to the shrub. This discrepancy may be due to differences in stressors affecting forests in both geographic regions such as strong tidal flow in Australia and high salinity or nutrient scarcity in Saudi Arabia (67).

Most notable was the difference in variation of alpha diversity metrics between depths of the fringe and the shrub. While the respective diversity metric was fairly consistent between depths in the fringe, it varied more strongly in the shrub, generally showing higher values at the surface (68). The higher variability between depths in the shrub was similarly highlighted by the relative abundance of phyla between sites indicating a more diverse bacterial community in shrub soils compared to the soils of tall fringing mangroves. The ordination analysis also shows this diversification in the shrub samples of both geographic regions. While the samples from the fringe grouped together tightly, the shrub samples show more heterogeneity in their spatial arrangement. All these diversity measures clearly show an increased diversification of the bacterial community in the shrub forest, regardless of its geographic location, which can be explained by the reduced hydrodynamic forcing in the high intertidal (69). Selective forces in habitats in which dispersal limitation prevails may be the driving factors of this diversification as has been discussed in other studies (39, 40, 70). The differing results at ASV compared to genus level indicate a potential impact of local environmental and evolutionary factors on bacterial community assembly over geographic distance. At ASV level the geographic region was the second strongest explanatory factor (Fig. 2C; Table S8), while it lost its explanatory strength when analyzed at genus level. Instead, the local factor depth became more important in separating the data in ordination space (Fig. 2D; Table S10). This indicates a similarity at a higher taxonomic level (genus), which diversifies differently between the geographic regions at the finest taxonomic scale (ASV). Such various levels of taxonomic resolution have been shown to change the level of differentiation between bacterial communities (63, 71), which has been hypothesized to be due to evolutionary factors such as genetic drift and/or speciation (40). The importance in acknowledging the taxonomic resolution (or taxonomic depth) when searching for biogeographic patterns has been highlighted before (72, 73) and may be an important factor in disentangling mechanisms driving microbial community assembly (40).

Global patterns: distance and historical contingency. While the local environmental factors were dominant in shaping the bacterial community composition, our results also provide evidence for differences between the bacterial communities of geographically distant mangrove forests. These findings contradict the traditional paradigm of “everything is everywhere” (74), which supports the theory of microbiological cosmopolitanism (75), in favor of the contemporary approach of an interplay of contrasting assembly mechanisms (37–40). The higher number of observed ASVs in Saudi Arabia, which is supported by higher phylogenetic diversity, may stem from the less favorable conditions for growth such as oligotrophy, higher levels of carbonates, high salinity, and extreme temperatures in the Red Sea (76, 77). These conditions along with a small tidal range (0.2 m) in Saudi Arabia which may limit dispersal (78, 79), can

enhance the effects of environmental selection. Because we did not observe strong separation of bacterial communities at genus level among geographic regions suggests that evolutionary processes such as genetic drift or speciation may be in place (40). Speciation is considered to have a negligible effect in communities that are connected via dispersal (61, 80, 81), but may influence bacterial communities that are separated by environmental boundaries (82–84).

Network analysis. The results from our co-occurrence network analysis show that community composition is not directly linked to network structure, as the networks clearly differ more among the geographic regions compared to local factors. In particular, the bacterial networks in Australian soils appear smaller, yet more closely connected in comparison with Saudi Arabian networks. The lower modularity and higher centralization values of the Australian networks suggest a network structure that is built around a few well-connected nodes. In contrast, in Saudi Arabia, the networks support a larger number of nodes that hold a central position (decentralized), with more independent functional modules. The difference in network structure among geographic regions may be due to the generally nutrient poor conditions, high water temperatures, and seasonal fluctuations (leading to long periods of desiccation) in Saudi Arabia (77) which may create an environment that promotes the formation of multiple functionally isolated groups of bacteria.

Important phyla for the connectedness of the networks were identified, including *Cyanobacteria*, *Gemmatimonadetes*, *Zixibacteria*, and *Spirochaetes*. The high betweenness values of *Cyanobacteria* in surface samples suggests the possible importance of this phylum in regulating the occurrence or absence of clusters of co-occurring bacteria within soils. Such a role has previously been suggested for *Cyanobacteria* in different environments, for example in desert soils (85). The regulating role of *Cyanobacteria* may be due to their ability to synthesize C- and N-rich organic compounds in nutrient limited conditions (86), or the formation of tightly connected mats which can select for or inhibit other bacteria (87). Their importance in the surface samples of the shrub in Australia was particularly pronounced, where they were the only phylum with a high node degree score (Fig. 4). This stands in contrast to the relative abundance of *Cyanobacteria* which is higher in Saudi Arabia than in Australia (Fig. S8). In Saudi Arabia resource scarcity may have supported high relative numbers of *Cyanobacteria* in the surface layers of the sediment but in Australia they were more important in structuring the network topology.

The dominant role of the phylum *Gemmatimonadetes* in facilitating connections between and within modules (as shown by high betweenness and high topological coefficient) is difficult to interpret since limited physiological information on this Phylum is available (88). *Gemmatimonadetes* were first described in 2003 (89), even though they are routinely detected in culture independent sequencing approaches and comprise about 2% of terrestrial soil communities (90). However, they have been proposed as oligotrophs with the potential of degrading complex organic material (OM), which is often present in high concentrations in mangrove soils (91). Their role as seen in the network structure may therefore be the degradation of more complex carbon substrates into smaller fractions, making these readily available for modules of bacteria to utilize. *Zixibacteria*, also a recently described phylum (92), were well connected within modules of many networks, as indicated by high topological coefficient scores. The metabolism of *Zixibacteria* has been suggested as highly versatile and adaptable to fluctuating environmental conditions (92, 93). The identification of genes potentially encoding nitrite/nitrate oxidoreductase (NXR), an important enzyme of the nitrification pathway, that has also been proposed to function as a nitrate reductase in anammox organisms, highlights a potentially important role of *Zixibacteria* in the nitrogen cycle of mangrove soils under aerobic or anaerobic conditions (92, 94). In deep sea sites of hydrocarbon seepage, *Zixibacteria* have been found to be the dominant fermenters of organic material, making OM more accessible for further degradation (95). The plasticity of metabolic pathways proposed for *Zixibacteria* may be the reason for

high co-occurrence rates of this phylum within tightly knit groups of other phyla within the network structure. A similar role of fermentation of OM may be played by bacteria of the phylum *Spirochaetes*, which have been shown to recycle necromass in polluted habitats, thereby providing substrates for further OM breakdown such as sulfate reduction (96, 97). Interestingly, the most abundant phylum across all samples, *Proteobacteria*, did not play an important role in the structure of the constructed co-occurrence networks. This was also the case for the next most abundant phylum *Bacteroidetes*. The phyla identified as creating the most important inter- and intramodule connectivity, were those with comparably low relative abundances such as *Zixibacteria*, *Gemmatimonadetes*, and *Spirochaetes*. This finding underlines the rare taxa concept, that high abundance of a taxa is not a sign of its importance within the community (98, 99). Instead, taxa of low abundance but high connectedness can have a large influence on the facilitation of processes within the community (44, 100, 101). Overall, the topological parameters of the networks, separated by phylum, were unable to identify differences between the factors of this study.

The relative distribution of node degrees between phyla, which indicates the connectedness of phyla within the network, displayed distinct differences between the two geographic regions. In Australia, nodes with high degrees (>250) were almost exclusively dominated by a small number of phyla, indicating the disproportional importance of single phyla in those networks. In contrast, the Saudi Arabian soils featured a highly diverse assemblage of phyla contributing to the connectedness of the networks. This may be due to the strongly limiting conditions in Saudi Arabian mangroves, which require a diverse set of metabolic pathways to utilize the scarce resources present. The contrasting effects that different levels of stress can exert on microbial interactions have been discussed in the light of the intermediate stress hypothesis (102, 103) and the stress gradient hypothesis (67). In this study, it is likely that the nature of the local stressors differs between the two geographic regions, resulting in different profiles of community interaction.

Functional implications. The identified functional groups (assigned by FAPROTAX) differed mainly between local factors. "Respiration of sulfur compounds" was highly abundant in all sites. Metabolic pathways of the sulfur cycle are vital components of many marine sediments, including mangrove soils; sulfate respiration is one of the major respiration pathways in anoxic soils (104, 105), and is said to reduce methane emissions from intertidal soils by outcompeting methanotrophs in high salinity and sulfate-rich conditions (106, 107). "Chemoheterotrophy" was different between depths, probably separated along the soil profile by oxygen availability. The high abundance of chemoheterotrophs demonstrates the prominent heterotrophic bacterial community, which is supported by organic rich soils (108). Chemoheterotrophy has been described as a method of carbon recycling in microbial communities of marine soils (109). Chemoheterotrophic expression was notably higher in the surface of the shrub in Saudi Arabia compared to the Australian shrub sites, which may further suggest a more efficient reuse of the available resources in a system with low tidal exchange. Functions related to primary productivity, such as "photoautotrophy," "cyanobacteria" (grouped as a function by FAPROTAX), and "oxygenic photoautotrophy" were most different between the surface and the subsurface. Light is essential for phototrophy to take place, and most likely the main driver in this separation.

These functional assignments are based on the literature rather than gene expression or metabolic measurements and can only suggest possibly active functions within the sampled communities (110). In a comparative study such as this one, functional assignment can nevertheless be a relevant addition to the analysis of the bacterial communities and shed light on the contrasting metabolic pathways in different parts of the forest.

CONCLUSION

Our findings suggest that the environmental parameters shaping the local soil environment are more important in determining the composition of the soil bacterial

community than geographic distance. However, this study also shows that geographic differentiation of the bacterial community is evident when investigated at the finest taxonomic resolution. The extent to which this variability is of functional importance needs to be assessed in future studies.

This work supports the importance of environmental selection as a driving process in microbial community assembly. Therefore, considering and accounting for local variability in environmental conditions, including the physical dynamics, is eminent when planning for mangrove restoration and scientific assessment of biogeochemical functions (e.g., carbon sequestration and nutrient processing). Understanding the spatial variability and distribution of microbial communities in mangrove soils, as well as their ecological functions, is important in order to predict changes and mitigate the impacts of intensified anthropogenic pressures and climate change (12, 20, 111, 112).

MATERIALS AND METHODS

Site descriptions and experimental design. Sampling was conducted in two arid monospecific mangrove forests of *A. marina*, at two distant geographic regions: on the central west coast of Australia, near Exmouth (22.49° S; 114.33° E), and in the central Red Sea, on the western coast of Saudi Arabia, near Thuwal (22.33° N; 39.09° E) (Fig. 6). These regions lie approximately 9,500 km apart, on the southern and northern boundaries of the tropics, respectively, and share certain climatological characteristics, including low mean annual rainfall (249 mm and 54 mm, respectively) and high mean annual maximum temperatures (32.0°C and 36.3°C, respectively) (<http://reg.bom.gov.au/climate/data/>; <http://www.saudi-arabia.climateemps.com/>). The tidal range, however, differed substantially between the two geographic regions where the mean range in Australia (2 m) is about 1 order of magnitude higher than in Saudi Arabia (0.2 m). Sampling was conducted in June 2018 in Australia and in December 2018 in Saudi Arabia, hence during the winter season in both regions.

In both geographic regions, two contrasting sites were chosen to encompass variation in their hydrographic conditions. The sheltered sites were situated inside embayments that shielded them from the direct exposure to the open sea. The exposed sites face the open sea with direct exposure to wave/wind action and stronger oceanic influence. At each site, samples were collected from the tall fringe and dwarfed shrub zones of the mangrove forest, and each sample was split into two depth segments.

Six cores per zone were collected from Australian mangrove soils due to limited resources, while nine cores were sampled per zone in Saudi Arabia (as triplicates of each nested location; see Fig. 6). Cores were taken using a 60 ml polyethylene syringe with cutoff tip (3 cm diameter), that extended approximately 10 cm into the soil. All cores were subsequently separated into surface (0–2 cm) and subsurface (5–7 cm) fractions. The soil depths at the exposed site in Saudi Arabia were very shallow (max. 5 cm), due to an underlying hard carbonate platform. In these environments, the deepest possible depth was sampled (3–5 cm). All samples were kept in the dark on ice and taken to the laboratory for storage at –80°C, immediately after the sampling was completed (2–3 h). Across geographic regions (Saudi Arabia/Australia), coastal exposures (exposed/sheltered), forest zones (fringe/shrub), and soil depths (surface/subsurface), a total of 120 samples were collected (of which 5 were later discarded during analysis).

DNA extraction and target gene amplification. DNA for bacterial community analysis was extracted from approximately 0.8 g of soil, using the DNeasy PowerSoil kit (Qiagen, Hilden, Germany). Using the specific primers 341F and 805R (113) with overhang illumina adapters (Illumina Inc., San Diego, CA, USA), the V3-V4 hypervariable regions of the 16S rRNA gene were amplified by PCR (PCR), at a final reaction volume of 25 μ l per sample (114). The amplified samples were cleaned to remove primer-dimers and nontargeted DNA molecules using the SequalPrep Normalization Plate kit (Invitrogen, Carlsbad, CA, USA). Library preparation was carried out using the Nextera XT Index kit (Illumina Inc., San Diego, CA, USA) in combination with the Qiagen Multiplex PCR Master Mix (Qiagen, Hilden, Germany) that uses the HotStarTaq DNA polymerase. The cyclor was set to 95°C as initial temperature for 15 min, followed by 8 cycles of 95°C for 30 s, 55°C for 90 s, and 72°C for 30 s, and a final extension with 95°C for 5 min (as specified by the manufacturer), before a second cleanup and normalization step was performed (SequalPrep Normalization Plate [96] kit, Invitrogen, Carlsbad, CA, USA). The libraries were then concentrated by vacuum centrifugation to approximately 12–15 nM, their concentration was measured by qPCR, and the amplicon length was validated with a Bioanalyzer at the KAUST Bioscience Core Lab. The samples were then sequenced on the Illumina MiSeq platform - v3 chemistry - (Illumina Inc., San Diego, CA, USA) with paired-end sequencing over 301 cycles.

Bioinformatics. The PCR primer sequences were removed from the dereplicated reads using the cutadapt software v. 2.1 (115) with a max error rate of 7%. Untrimmed sequences were removed. The DADA2 software package v. 1.10 (116) was used to differentiate exact amplicon sequence variants (ASVs) and remove chimeras. Filtering parameters used were: maxN = 0, maxEE = c (3, 6), truncLen = c (260, 190), truncQ = 2. DADA2's core algorithm models the errors in Illumina-sequenced reads and assigns ASVs with an accuracy of two base pairs (bp) difference, based on the quality score distribution (116). ASVs have been proposed as a new method to group Illumina sequencing reads according to exact matches rather than arbitrarily chosen similarity thresholds (116), providing reproducibility of marker gene-based studies, and simultaneously maximizing the biological variation that can be captured in

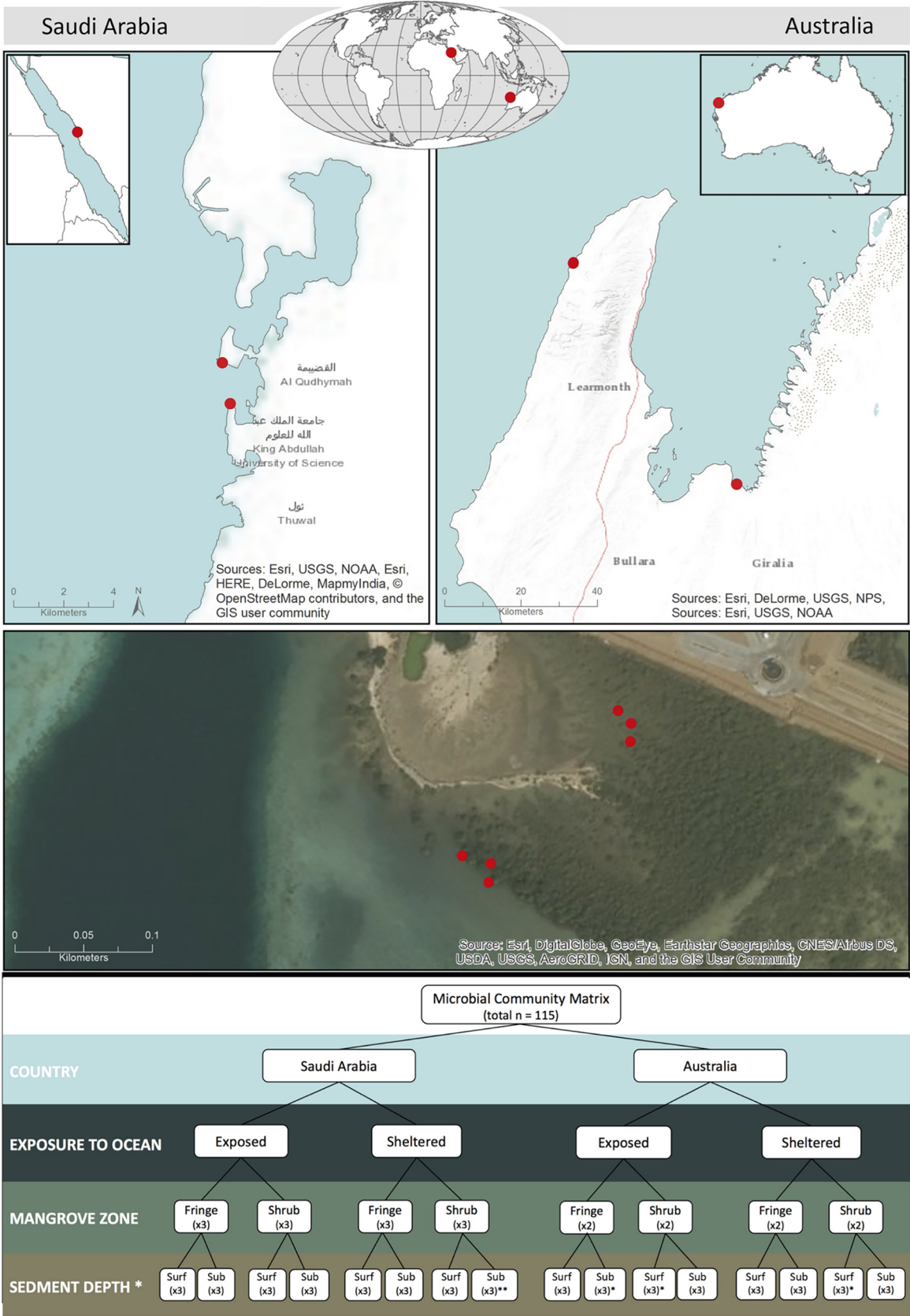


FIG 6 Map and sampling design of the nested factors. World map showing the global regions of the sampling sites on the Western Australian coast and in Saudi Arabia. The more detailed maps show the exposed and the sheltered sites in both geographic regions. An (Continued on next page)

each sample (117). The resulting ASVs were used for taxonomic classification using the SILVA database v. 132 (118). Eukaryotic and archaeal amplification artifacts that were also targeted by the relatively unspecific range of the V3-V4 primers used, were removed from the data set for downstream analysis. Rare ASVs (prevalence threshold of <0.5% relative to the total abundance of ASVs) were removed. Analysis of the “clean practices” negative controls identified two potentially contaminated samples. These samples showed significantly higher numbers of *Pluralibacter* and *Pseudomonas* (which are both common sources of cross-contamination in research laboratories) compared to the other samples but were still below 5% and 0.5% prevalence of all sequences of either sample, respectively. The samples were therefore omitted from further analysis. Samples that contained < 5000 reads were removed, and the remaining samples were rarefied to the minimum depth of 6048 sequences per sample (R package phyloseq v. 1.26.1, seed = 33) (119). In total, five samples (three from Australia, two from Saudi Arabia) were discarded due to insufficient sequencing depth (0, 0, 3517 sequences), and possible cross-contamination. Sequences were aligned (R package DECIPHER v 2.12.0) (120) for phylogenetic tree construction (R package phangorn v 2.5.5) (121), from which the alpha diversity metric of phylogenetic diversity (Faith's PD) was calculated (R package picante v 1.8.2) (122). From an initial number of 13,972,966 raw sequences, 10,200,365 sequences were retained after trimming and quality filtering. After merging forward and reverse reads, 4,271,706 sequences remained and after chimera removal a final 3,890,485 sequences remained. After filtration of erroneous sequences (archaeal, chloroplast, or mitochondrial sequences) and removal of rare ASVs (5% prevalence threshold), the abundance table contained 3,657 ASVs across 115 samples (Table S1). The asymptotic rarefaction curves of each sample show that the majority of the taxonomic diversity was covered sufficiently by the sequencing depth and suggested a rarefaction threshold of 5,000 sequences per sample (Fig. S1 and S2). Agglomeration of samples to the phylum and genus level resulted in 37 unique phyla and 233 genera (Table S2).

Network analysis. To identify ecological co-occurrence patterns in the bacterial communities, a co-occurrence network was generated for each combination of geographic region, exposure, zone, and depth using the CoNet plugin of Cytoscape 3.4 (123–125) and Gephi 0.9.1 (126) for computation and visualization, respectively. We focused on the phylotypes present in each distinct location to identify co-occurring taxa within networks that could possibly indicate functional/physical interactions in the environment (49). A combination of the Bray-Curtis (BC) and Kullback-Leiber (KLD) dissimilarity indices, along with the Pearson and Spearman correlation coefficients were used to build the networks. Edge-specific permutation and bootstrap score distributions with 1,000 iterations were performed. For each measure and edge, 100 permutations and bootstrap scores were generated. The resulting data were normalized to detect statistically significant non-random events of co-occurrences (i.e., co-presences and mutual exclusions). The *P* values were computed by z-scoring the permuted null and bootstrap confidence intervals using pooled variance (127). The most important statistical network descriptors that describe the overall structure of the network (Clustering coefficient, Centralization, Diameter, Average Neighbors, Density) were calculated using the Network Analyzer in Cytoscape (128) and the number of modules (resolution 2.5) were determined using Gephi 0.9.1.

The bacterial ASVs were represented as nodes (the central elements in the networks), from which most network parameters are calculated. Edges meanwhile represent the connections or links between the nodes, which can co-occur or be mutually exclusive. In undirected networks, such as these, no assumptions are made as to which node facilitates the presence or absence of a neighboring node. The degree of a node denotes the number of edges connecting it to other nodes, giving it a direct value of connectedness and therefore communicative importance within the network. A module is defined as a substructure within the network that exhibits a higher level of connectivity between its members compared to other members of the same network and can be used as a measure of compartmentalization of the network. Betweenness centrality can be interpreted as a measure of relevance of a node in connecting functional modules (strongly connected groups of nodes) of bacteria, with a higher score indicating an elevated importance in facilitating such a connection. Betweenness centrality can be a stronger representation of an important connection within a network, since it favors nodes that join interconnected communities rather than single nodes. The topological coefficient is a relative measure to which extent a node shares neighbors with other nodes. It therefore shows the relative connectedness of a node within its module as opposed to the entire network. Hence, nodes with a high topological coefficient are central to their module, possibly by creating an environment suitable for their co-occurring neighbors. Network analysis can also be used to identify keystone taxa (46). These are highly connected taxa that facilitate the connectivity in the network, and thereby have an increased influence on the structure and functioning of the microbial community (44).

Functional assignments. The Functional Annotation of Prokaryotic taxa (FAPROTAX) database v. 1.2.1 (110) was used to perform functional annotation of the ASVs according to literature references of known microbial metabolism. The functions were assigned to the ASV table containing taxonomic annotations (from SILVA database), using the python script “collapse_table.py” in python v. 3.7.4 (129). A total of 1103 ASVs out of 3491 ASVs (30.7%) were assigned to 40 functions (out of 90 possible). Fifteen func-

FIG 6 Legend (Continued)

aerial photograph visualizes the separation between the zones of each forest, with actual sampling locations at the sheltered site in Saudi Arabia separated into three plots each at the tall fringe and the shrub as an example for sampling separation within each of the zones. The schematic representation of the sampling design below, shows the arrangement of the experimental factors and the numbers of replicates taken. The values in brackets represent the number of replicates for each sample. The numbers in the last row denote the sampling depth of the surface 0–2 cm (Surf) and the subsurface 2–10 cm (Sub). Asterisks (*) represents from which site a sample that has been removed for insufficient sequencing depth or cross-contamination, making the total number of samples *n* = 115.

tions were removed due to redundancy (“aerobic chemoheterotrophy” was removed in favor of “chemoheterotrophy”) if they aligned collinearly (>80%), or low prevalence (if appeared in three or less samples), resulting in a set of 25 assigned functions.

Statistical analysis. All statistical analyses were performed in R v. 3.6.1 (130), using the phyloseq v. 1.26.1 (119) and vegan v. 2.5.6 (131) packages and all graphs were created using ggplot2 v. 3.2.1 (132). Our explanatory variable structure consists in four categorical variables: “geographic region” (fixed and orthogonal; 2 levels: Australia and Saudi Arabia); “exposure” (fixed and orthogonal; 2 levels: exposed and sheltered); “zone” (fixed and orthogonal; 2 levels: fringe and shrub); “depth” (fixed and orthogonal; 2 levels: surface and subsurface). Two alpha diversity metrics, i.e., observed number of ASVs and Shannon diversity index, were calculated with phyloseq and differences between factors were tested using analysis of variance (ANOVA) after validating the normal distribution of residuals and homoscedasticity. Differences in Faith’s PD between experimental factors were tested using ANOVA. Variance partitioning of the abundance matrix (log + 1 transformed) with respect to the factors was performed with the varpart() function in “vegan” and its significance was tested by redundancy analysis (RDA). Beta-diversity at two taxonomic levels (ASV, genus) was visualized by nonmetric multidimensional scaling (NMDS), using a Bray-Curtis dissimilarity matrix estimated from the square-root-transformed and Wisconsin double-standardized ASV table. Canonical Analysis of Principal components (CAP) was performed in Primer v6 (133). A permutational multivariate analysis of variance (PERMANOVA; permutations = 999, distance = Bray-Curtis) was performed on the log transformed abundance matrix after checking the homogeneity of multivariate dispersion, to test the difference of bacterial community composition among the factors of our experimental design. PERMANOVA (permutations = 999, distance = Bray-Curtis) was conducted to test for differences of functional assignments between factors according to the design presented above.

Data availability. The raw sequence data were deposited in the SRA of the NCBI (<https://www.ncbi.nlm.nih.gov/sra>) under accession number PRJNA720541.

SUPPLEMENTAL MATERIAL

Supplemental material is available online only.

SUPPLEMENTAL FILE 1, PDF file, 4.9 MB.

ACKNOWLEDGMENTS

We thank Eleonora Fossile for her assistance during the DNA extractions, Ute Langner for creation of the map, Jonas Thomson for the graphical assembly of the figure panels, and the editor and the anonymous reviewers whose comments have resulted in a much-improved manuscript.

T.T., M.F., S.C., C.E.L., and J.I.E. contributed to the conceptualization and design of the study. T.T., M.B.S., N.P., E.A., and J.I.E. conducted field work and laboratory analyses. T.T., M.F., E.A., and J.I.E. analyzed the data. C.E.L. and B.H.J. supported the project financially and supervised it. T.T., M.F., J.I.E. wrote the manuscript and all authors read and approved the final version of it.

This work was funded by KAUST baseline funding to B.H.J. as well as baseline funding from University of Queensland to C.E.L. A travel grant from the Red Sea Research Centre (RSRC) at KAUST was awarded to T.T. This research received no specific grant from any funding agency in the public, commercial, or nonprofit sectors.

REFERENCES

- Donato DC, Kauffman JB, Murdiyarso D, Kurnianto S, Stidham M, Kanninen M. 2011. Mangroves among the most carbon-rich forests in the tropics. *Nature Geosci* 4:293–297. <https://doi.org/10.1038/ngeo1123>.
- Alongi DM. 2020. Global significance of mangrove blue carbon in climate change mitigation. *Sci* 2:67. <https://doi.org/10.3390/sci2030067>.
- Alongi DM. 1994. The role of bacteria in nutrient recycling in tropical mangrove and other coastal benthic ecosystems. *Hydrobiologia* 285: 19–32. <https://doi.org/10.1007/BF00005650>.
- Alongi DM. 1988. Bacterial productivity and microbial biomass in tropical mangrove sediments. *Microb Ecol* 15:59–79. <https://doi.org/10.1007/BF02012952>.
- Holguin G, Vazquez P, Bashan Y. 2001. The role of sediment microorganisms in the productivity, conservation, and rehabilitation of mangrove ecosystems: an overview. *Biol Fertil Soils* 33:265–278. <https://doi.org/10.1007/s003740000319>.
- Soldan R, et al. 2019. Bacterial endophytes of mangrove propagules elicit early establishment of the natural host and promote growth of cereal crops under salt stress. *Microbiol Res*. <https://doi.org/10.1016/j.MICRES.2019.03.008>.
- Alongi DM. Mangrove-microbe-soil relations. 85–103 2005
- Reef R, Feller IC, Lovelock CE. 2010. Nutrition of mangroves. *Tree Physiol* 30:1148–1160. <https://doi.org/10.1093/treephys/tpq048>.
- Trevathan-Tackett SM, Sherman CDH, Huggett MJ, Campbell AH, Laverock B, Hurtado-McCormick V, Seymour JR, Firl A, Messer LF, Ainsworth TD, Negandhi KL, Daffonchio D, Egan S, Engelen AH, Fusi M, Thomas T, Vann L, Hernandez-Agreda A, Gan HM, Marzinelli EM, Steinberg PD, Hardtke L, Macreadie PI. 2019. A horizon scan of priorities for coastal marine microbiome research. *Nat Ecol Evol* 3:1509–1520. <https://doi.org/10.1038/s41559-019-0999-7>.
- Thompson LR, Sanders JG, McDonald D, Amir A, Ladau J, Locey KJ, Prill RJ, Tripathi A, Gibbons SM, Ackermann G, Navas-Molina JA, Janssen S, Kopylova E, Vázquez-Baeza Y, González A, Morton JT, Mirarab S, Zech Xu Z, Jiang L, Haroon MF, Kanbar J, Zhu Q, Jin Song S, Kosciulek T, Bokulich NA, Lefler J, Brislawn CJ, Humphrey G, Owens SM, Hampton-Marcell J, Berg-lyons D, McKenzie V, Fierer N, Fuhrman JA, Clausen A, Stevens RL, Shade A, Pollard KS, Goodwin KD, Jansson JK, Gilbert JA, Knight R, Earth Microbiome Project Consortium. 2017. A communal catalogue reveals Earth’s multiscale microbial diversity. *Nature* 551:457–463. <https://doi.org/10.1038/nature24621>.

11. Bahram M, Hildebrand F, Forslund SK, Anderson JL, Soudzilovskaia NA, Bodegom PM, Bengtsson-Palme J, Anslan S, Coelho LP, Harend H, Huerta-Cepas J, Medema MH, Maltz MR, Mundra S, Olsson PA, Pent M, Pölme S, Sunagawa S, Ryberg M, Tedersoo L, Bork P. 2018. Structure and function of the global topsoil microbiome. *Nature* 560:233–237. <https://doi.org/10.1038/s41586-018-0386-6>.
12. Cavicchioli R, et al. 2019. Scientists' warning to humanity: microorganisms and climate change. *Nat Rev Microbiol*. <https://doi.org/10.1038/s41579-019-0222-5>.
13. Ferreira TO, Otero XL, de Souza Junior VS, Vidal-Torrado P, Macías F, Firme LP. 2010. Spatial patterns of soil attributes and components in a mangrove system in Southeast Brazil (São Paulo). *J Soils Sediments* 10: 995–1006. <https://doi.org/10.1007/s11368-010-0224-4>.
14. Odum WE, Heald EJ. 1975. Mangrove forests and aquatic productivity, p 129–136. *In* Coupling of land and water systems. Springer, Berlin, Heidelberg. https://doi.org/10.1007/978-3-642-86011-9_5.
15. Odum WE, Heald EJ. 1975. The detritus-based food web of an estuarine mangrove community, p 738. *In* Estuarine research: volume I, chemistry, biology, and the estuarine system. Academic Press, Inc.
16. Moitinho MA, Bononi L, Souza DT, Melo IS, Taketani RG. 2018. Bacterial succession decreases network complexity during plant material decomposition in mangroves. *Microb Ecol* 76:954–963. <https://doi.org/10.1007/s00248-018-1190-4>.
17. Clark MW, McConchie D, Lewis DW, Saenger P. 1998. Redox stratification and heavy metal partitioning in Avicennia-dominated mangrove sediments: a geochemical model. *Chem Geol* 149:147–171. [https://doi.org/10.1016/S0009-2541\(98\)00034-5](https://doi.org/10.1016/S0009-2541(98)00034-5).
18. Penha-Lopes G, Kristensen E, Flindt M, Mangion P, Bouillon S, Paula J. 2010. The role of biogenic structures on the biogeochemical functioning of mangrove constructed wetlands sediments – A mesocosm approach. *Mar Pollut Bull* 60:560–572. <https://doi.org/10.1016/j.marpolbul.2009.11.008>.
19. Booth JM, Fusi M, Marasco R, Bobo T, Daffonchio D. 2019. Fiddler crab bioturbation determines consistent changes in bacterial communities across contrasting environmental conditions. *Sci Rep* 9:3749. <https://doi.org/10.1038/s41598-019-40315-0>.
20. Kuramae EE, Yergeau E, Wong LC, Pijl AS, van Veen JA, Kowalchuk GA. 2012. Soil characteristics more strongly influence soil bacterial communities than land-use type. *FEMS Microbiol Ecol* 79:12–24. <https://doi.org/10.1111/j.1574-6941.2011.01192.x>.
21. Feller IC, McKee KL, Whigham DF, O'Neill JP. 2003. Nitrogen vs. phosphorus limitation across an ecotonal gradient in a mangrove forest. *Biogeochemistry* 62:145–175. <https://doi.org/10.1023/A:1021166010892>.
22. Lovelock CE, Feller IC, McKee KL, Thompson R. 2005. Variation in mangrove forest structure and sediment characteristics in Bocas del Toro. *Panama Caribbean J Sci* 41:456–464.
23. Holguin G, Gonzalez-Zamorano P, de-Bashan LE, Mendoza R, Amador E, Bashan Y. 2006. Mangrove health in an arid environment encroached by urban development—a case study. *Sci Total Environ* 363:260–274. <https://doi.org/10.1016/j.scitotenv.2005.05.026>.
24. Feller IC, Lovelock CE, McKee KL. 2007. Nutrient addition differentially affects ecological processes of Avicennia germinans in nitrogen versus phosphorus limited mangrove ecosystems. *Ecosystems* 10:347–359. <https://doi.org/10.1007/s10021-007-9025-z>.
25. Feller IC, Lovelock CE, Berger U, McKee KL, Joye SB, Ball MC. 2010. Bio-complexity in mangrove ecosystems. *Annu Rev Mar Sci* 2:395–417. <https://doi.org/10.1146/annurev.marine.010908.163809>.
26. Gonzalez-Acosta B, Bashan Y, Hernandez-Saavedra NY, Ascencio F, Cruz-Agüero G. 2006. Seasonal seawater temperature as the major determinant for populations of culturable bacteria in the sediments of an intact mangrove in an arid region. *FEMS Microbiol Ecol* 55:311–321. <https://doi.org/10.1111/j.1574-6941.2005.00019.x>.
27. Gomes NCM, Flocco CG, Costa R, Junca H, Vilchez R, Pieper DH, Krögerrecklenfort E, Paranhos R, Mendonça-Hagler LCS, Smalla K. 2010. Mangrove microniches determine the structural and functional diversity of enriched petroleum hydrocarbon-degrading consortia. *FEMS Microbiol Ecol* 74:276–290. <https://doi.org/10.1111/j.1574-6941.2010.00962.x>.
28. Vera-Gargallo B, Chowdhury TR, Brown J, Fansler SJ, Durán-Viseras A, Sánchez-Porro C, Bailey VL, Jansson JK, Ventosa A. 2019. Spatial distribution of prokaryotic communities in hypersaline soils. *Sci Rep* 9:1769. <https://doi.org/10.1038/s41598-018-38339-z>.
29. Andreote FD, Jiménez DJ, Chaves D, Dias ACF, Luvizotto DM, Dini-Andreote F, Fasanella CC, Lopez MV, Baena S, Taketani RG, de Melo IS. 2012. The Microbiome of Brazilian mangrove sediments as revealed by metagenomics. *PLoS One* 7:e38600. <https://doi.org/10.1371/journal.pone.0038600>.
30. Imchen M, Kumavath R, Barh D, Azevedo V, Ghosh P, Viana M, Wattam AR. 2017. Searching for signatures across microbial communities: meta-genomic analysis of soil samples from mangrove and other ecosystems. *Sci Rep* 7:8859. <https://doi.org/10.1038/s41598-017-09254-6>.
31. Imchen M, Kumavath R, Barh D, Vaz A, Góes-Neto A, Tiwari S, Ghosh P, Wattam AR, Azevedo V. 2018. Comparative mangrove metagenome reveals global prevalence of heavy metals and antibiotic resistance across different ecosystems. *Sci Rep* 8:11187. <https://doi.org/10.1038/s41598-018-29521-4>.
32. Zhu P, Wang Y, Shi T, Zhang X, Huang G, Gong J. 2018. Intertidal zonation affects diversity and functional potentials of bacteria in surface sediments: a case study of the Golden Bay mangrove, China. *Appl Soil Ecol* 130:159–168. <https://doi.org/10.1016/j.apsoil.2018.06.003>.
33. Zhu P, Wang Y, Shi T, Huang G, Gong J. 2018. Genetic diversity of benthic microbial eukaryotes in response to spatial heterogeneity of sediment geochemistry in a mangrove ecosystem. *Estuaries and Coasts* 41: 751–764. <https://doi.org/10.1007/s12237-017-0317-z>.
34. Chen Q, Zhao Q, Li J, Jian S, Ren H. 2016. Mangrove succession enriches the sediment microbial community in South China. *Sci Rep* 6:27468. <https://doi.org/10.1038/srep27468>.
35. Tavares TCL, Bezerra WM, Normando LRO, Rosado AS, Melo VMM. 2021. Brazilian semi-arid mangroves-associated microbiome as pools of richness and complexity in a changing world. *Front Microbiol* 12:1–18.
36. Zhang Z, Pan J, Pan Y, Li M. 2021. Biogeography, assembly patterns, driving factors, and interactions of archaeal community in mangrove sediments. *mSystems* 6:e01381–20. <https://doi.org/10.1128/mSystems.01381-20>.
37. Vellend M. 2010. Conceptual synthesis in community ecology. *Q Rev Biol* 85:183–206. <https://doi.org/10.1086/652373>.
38. Nemergut DR, Schmidt SK, Fukami T, O'Neill SP, Bilinski TM, Stanish LF, Knelman JE, Darcy JL, Lynch RC, Wickey P, Ferrenberg S. 2013. Patterns and processes of microbial community assembly. *Microbiol Mol Biol Rev* 77:342–356. <https://doi.org/10.1128/MMBR.00051-12>.
39. Martiny JBH, Bohannan BJM, Brown JH, Colwell RK, Fuhrman JA, Green JL, Horner-Devine MC, Kane M, Krumins JA, Kuske CR, Morin PJ, Naeem S, Ovreås L, Reysenbach A-L, Smith VH, Staley JT. 2006. Microbial biogeography: putting microorganisms on the map. *Nat Rev Microbiol* 4: 102–112. <https://doi.org/10.1038/nrmicro1341>.
40. Hanson CA, Fuhrman JA, Horner-Devine MC, Martiny JBH. 2012. Beyond biogeographic patterns: processes shaping the microbial landscape. *Nat Rev Microbiol* 10:497–506. <https://doi.org/10.1038/nrmicro2795>.
41. Langenheder S, Lindström ES. 2019. Factors influencing aquatic and terrestrial bacterial community assembly. *Environ Microbiol Rep* 11: 306–315. <https://doi.org/10.1111/1758-2229.12731>.
42. Pearson DE, Ortega YK, Eren Ö, Hierro JL. 2018. Community Assembly Theory as a Framework for Biological Invasions. *Trends Ecol Evol* 33: 313–325. <https://doi.org/10.1016/j.tree.2018.03.002>.
43. Li M, Mi T, He H, Chen Y, Zhen Y, Yu Z. 2021. Active bacterial and archaeal communities in coastal sediments: biogeography pattern, assembly process and co-occurrence relationship. *Sci Total Environ* 750:142252. <https://doi.org/10.1016/j.scitotenv.2020.142252>.
44. Banerjee S, Schlaeppi K, van der Heijden MGA. 2018. Keystone taxa as drivers of microbiome structure and functioning. *Nat Rev Microbiol* 16: 567–576. <https://doi.org/10.1038/s41579-018-0024-1>.
45. Banerjee S, Walder F, Büchi L, Meyer M, Held AY, Gatterger A, Keller T, Charles R, van der Heijden MGA. 2019. Agricultural intensification reduces microbial network complexity and the abundance of keystone taxa in roots. *ISME J* 13:1722–1736. <https://doi.org/10.1038/s41396-019-0383-2>.
46. Berry D, Widder S. 2014. Deciphering microbial interactions and detecting keystone species with co-occurrence networks. *Front Microbiol* 5: 219. <https://doi.org/10.3389/fmicb.2014.00219>.
47. Layeghifard M, Hwang DM, Guttman DS. 2017. Disentangling Interactions in the Microbiome: a Network Perspective. *Trends Microbiol* 25: 217–228. <https://doi.org/10.1016/j.tim.2016.11.008>.
48. Heleno R, Devoto M, Pocock M. 2012. Connectance of species interaction networks and conservation value: is it any good to be well connected? *Ecol Indic* 14:7–10. <https://doi.org/10.1016/j.ecolind.2011.06.032>.
49. Fuhrman JA. 2009. Microbial community structure and its functional implications. *Nature* 459:193–199. <https://doi.org/10.1038/nature08058>.
50. Pearman JK, Aylagas E, Voolstra CR, Anlauf H, Villalobos R, Carvalho S. 2019. Disentangling the complex microbial community of coral reefs using standardized Autonomous Reef Monitoring Structures (ARMS). *Mol Ecol* 28:3496–3507. <https://doi.org/10.1111/mec.15167>.
51. Tilman D. 2001. Functional diversity. *Encycl Biodivers* 109–120. <https://doi.org/10.1016/B0-12-226865-2/00132-2>.

52. Duke NC, Meynecke J-O, Dittmann S, Ellison AM, Anger K, Berger U, Cannicci S, Diele K, Ewel KC, Field CD, Koedam N, Lee SY, Marchand C, Nordhaus I, Dahdouh-Guebas F. 2007. A world without mangroves? *Science* 317:41–43. <https://doi.org/10.1126/science.317.5834.41b>.
53. Polidoro BA, Carpenter KE, Collins L, Duke NC, Ellison AM, Ellison JC, Farnsworth EJ, Fernando ES, Kathiresan K, Koedam NE, Livingstone SR, Miyagi T, Moore GE, Ngoc Nam V, Ong JE, Primavera JH, Salmo SG, Sanciangco JC, Sukardjo S, Wang Y, Yong JWH. 2010. The loss of species: mangrove extinction risk and geographic areas of global concern. *PLoS One* 5:e10095. <https://doi.org/10.1371/journal.pone.0010095>.
54. Saintilan N, Khan NS, Ashe E, Kelleway JJ, Rogers K, Woodroffe CD, Horton BP. 2020. Thresholds of mangrove survival under rapid sea level rise. *Science* 368:1118–1121. <https://doi.org/10.1126/science.aba2656>.
55. Adame MF. 2020. Mangroves in arid regions: ecology, threats, and opportunities. *Estuar Coast Shelf Sci*. <https://doi.org/10.1016/j.ecss.2020.106796>.
56. Leopold A, Marchand C, Deborde J, Chaduteau C, Allenbach M. 2013. Influence of mangrove zonation on CO₂ fluxes at the sediment-air interface (New Caledonia). *Geoderma* 202–203:62–70. <https://doi.org/10.1016/j.geoderma.2013.03.008>.
57. Fierer N, Jackson RB. 2006. The diversity and biogeography of soil bacterial communities. *Proc Natl Acad Sci U S A* 103:626–631. <https://doi.org/10.1073/pnas.0507535103>.
58. Hugerth LW, Larsson J, Alneberg J, Lindh MV, Legrand C, Pinhassi J, Andersson AF. 2015. Metagenome-assembled genomes uncover a global brackish microbiome. *Genome Biol* 16:279. <https://doi.org/10.1186/s13059-015-0834-7>.
59. Sunagawa S, Coelho LP, Chaffron S, Kultima JR, Labadie K, Salazar G, Djahanschiri B, Zeller G, Mende DR, Alberti A, Cornejo-Castillo FM, Costea PI, Cruaud C, d'Ovidio F, Engelen S, Ferrera I, Gasol JM, Guidi L, Hildebrand F, Kokoszka F, Lepoivre C, Lima-Mendez G, Poulain J, Poulos BT, Royo-Llonch M, Sarmiento H, Vieira-Silva S, Dimier C, Picheral M, Searson S, Kandels-Lewis S, Bowler C, de Vargas C, Gorsky G, Grimsley N, Hingamp P, Iudicone D, Jaillon O, Not F, Ogata H, Pesant S, Speich S, Stemmann L, Sullivan MB, Weissenbach J, Wincker P, Karsenti E, Raes J, Acinas SG, Bork P, Tara Oceans coordinators, et al. 2015. Ocean plankton. Structure and function of the global ocean microbiome. *Science* 348: 1261359. <https://doi.org/10.1126/science.1261359>.
60. Rocha LL, Colares GB, Nogueira VLR, Paes FA, Melo VMM. 2016. Distinct habitats select particular bacterial communities in mangrove sediments. *Int J Microbiol* 2016:3435809. <https://doi.org/10.1155/2016/3435809>.
61. Fodelianakis S, et al. 2019. Dispersal homogenizes communities via immigration even at low rates in a simplified synthetic bacterial metacommunity. *Nat Commun* 10:23955–26900.
62. Chen Y-J, Leung PM, Cook PLM, Wong WW, Hutchinson T, Eate V, Kessler AJ, Greening C. 2021. Hydrodynamic disturbance controls microbial community assembly and biogeochemical processes in coastal sediments. *ISME J* 1–14. <https://doi.org/10.1038/s41396-021-01111-9>.
63. Jiang X-T, Peng X, Deng G-H, Sheng H-F, Wang Y, Zhou H-W, Tam NF-Y. 2013. Illumina sequencing of 16S rRNA tag revealed spatial variations of bacterial communities in a mangrove wetland. *Microb Ecol* 66:96–104. <https://doi.org/10.1007/s00248-013-0238-8>.
64. Thrush SF, Gray JS, Hewitt JE, Uglund KI. 2006. Predicting the effects of habitat homogenization on marine biodiversity. *16(5):1636–42*.
65. Hewitt J, Thrush S, Lohrer A, Townsend M. 2010. A latent threat to biodiversity: consequences of small-scale heterogeneity loss. *Biodivers Conserv* 19:1315–1323. <https://doi.org/10.1007/s10531-009-9763-7>.
66. Vellend MARK, Verheyen KRIS, Flinn KM, Jacquemyn HANS, Kolb A, VAN Calster HANS, Peterken G, Graae BJ, Bellemare J, Honnay O, Brunet JÖRG, Wulf M, Gerhardt F, Hermy M. 2007. Homogenization of forest plant communities and weakening of species-environment relationships via agricultural land use. *J Ecol* 95:565–573. <https://doi.org/10.1111/j.1365-2745.2007.01233.x>.
67. Hernandez DJ, David AS, Menges ES, Searcy CA, Afkhami ME. 2021. Environmental stress destabilizes microbial networks. *ISME J* 15:1722–1734. <https://doi.org/10.1038/s41396-020-00882-x>.
68. Fierer N, Schimel JP, Holden PA. 2003. Variations in microbial community composition through two soil depth profiles. *Soil Biol Biochem* 35: 167–176. [https://doi.org/10.1016/S0038-0717\(02\)00251-1](https://doi.org/10.1016/S0038-0717(02)00251-1).
69. Montgomery JM, Bryan KR, Horstman EM, Mullarney JC. 2018. Attenuation of tides and surges by mangroves: contrasting case studies from New Zealand. *Water (Switzerland)* 10:1119. <https://doi.org/10.3390/w10091119>.
70. Lindström ES, Langenheder S. 2012. Local and regional factors influencing bacterial community assembly. *Environ Microbiol Rep* 4:1–9. <https://doi.org/10.1111/j.1758-2229.2011.00257.x>.
71. Bay SK, McGeoch MA, Gillor O, Wieler N, Palmer DJ, Baker DJ, Chown SL, Greening C. 2020. Soil bacterial communities exhibit strong biogeographic patterns at fine taxonomic resolution. *mSystems* 5. <https://doi.org/10.1128/mSystems.00540-20>.
72. Green J, Bohannan BJM. 2006. Spatial scaling of microbial biodiversity. *Trends Ecol E* 21:P501–507. <https://doi.org/10.1016/j.tree.2006.06.012>.
73. Ramette A, Tiedje JM. 2007. Biogeography: an emerging cornerstone of understanding prokaryotic diversity, ecology, and evolution. *Microb Ecol* 53:197–207. <https://doi.org/10.1007/s00248-005-5010-2>.
74. Becking LB. 1934. *Geobiologie of inleiding tot de milieukunde*. (W. P. Van Stockum & Zoon).
75. Fenchel T, Finlay BJ. 2004. The ubiquity of small species: patterns of local and global diversity. *Bioscience* 54:777. [https://doi.org/10.1641/0006-3568\(2004\)054\[0777:TUOSSP\]2.0.CO;2](https://doi.org/10.1641/0006-3568(2004)054[0777:TUOSSP]2.0.CO;2).
76. Acker J, Leptoukh G, Shen S, Zhu T, Kempler S. 2008. Remotely-sensed chlorophyll a observations of the northern Red Sea indicate seasonal variability and influence of coastal reefs. *J Mar Syst* 69:191–204. <https://doi.org/10.1016/j.jmarsys.2005.12.006>.
77. Carvalho S, Kürten B, Krokos G, Hoteit I, Ellis JI. 2019. The Red Sea. *World Seas an Environ Eval*: 49–74. <https://doi.org/10.1016/B978-0-08-100853-9.00004-X>.
78. McLachlan JR, Haghighi JM, Greig HS. 2019. Strong zonation of benthic communities across a tidal freshwater height gradient. *Freshw Biol* 64:1284–1294. <https://doi.org/10.1111/fwb.13304>.
79. Boehm AB, Yamahara KM, Sassoubre LM. 2014. Diversity and transport of microorganisms in intertidal sands of the California coast. *Appl Environ Microbiol* 80:3943–3951. <https://doi.org/10.1128/AEM.00513-14>.
80. Logares R, Deutschmann IM, Junger PC, Giner CR, Krabberød AK, Schmidt TSB, Rubinat-Ripoll L, Mestre M, Salazar G, Ruiz-González C, Sebastián M, de Vargas C, Acinas SG, Duarte CM, Gasol JM, Massana R. 2020. Disentangling the mechanisms shaping the surface ocean microbiota. *Microbiome* 8:1–17. <https://doi.org/10.1186/s40168-020-00827-8>.
81. Stegen JC, Lin X, Fredrickson JK, Chen X, Kennedy DW, Murray CJ, Rockhold ML, Konopka A. 2013. Quantifying community assembly processes and identifying features that impose them. *ISME J* 7:2069–2079. <https://doi.org/10.1038/ismej.2013.93>.
82. Fulthorpe RR, Roesch LFW, Riva A, Triplett EW. 2008. Distantly sampled soils carry few species in common. *ISME J* 2:901–910. <https://doi.org/10.1038/ismej.2008.55>.
83. Power JF, et al. 2018. Microbial biogeography of 925 geothermal springs in New Zealand. *Nat Commun* 9:1–12.
84. Whitaker RJ, Grogan DW, Taylor JW. 2003. Geographic barriers isolate endemic populations of hyperthermophilic archaea. *Science* 301: 976–978. <https://doi.org/10.1126/science.1086909>.
85. Valverde A, Makhallanyane TP, Seely M, Cowan DA. 2015. Cyanobacteria drive community composition and functionality in rock-soil interface communities. *Mol Ecol* 24:812–821. <https://doi.org/10.1111/mec.13068>.
86. Kumar M, Singh DP, Prabha R, Sharma AK. 2015. Role of cyanobacteria in nutrient cycle and use efficiency in the soil, P 163–171. In Rakshit A, Singh HB, & Sen A (ed), *Nutrient Use Efficiency: from Basics to Advance*. Springer. <https://doi.org/10.1007/978-81-322-2169-2>.
87. Stal LJ. 2012. Cyanobacterial and stromatolites, p 65–125. In *Ecology of Cyanobacteria II: their Diversity in Space and Time*. Springer Netherlands.
88. Hanada S, Sekiguchi Y. 2014. The phylum gemmatimonadetes, p 677–681. In *The Prokaryotes: other Major Lineages of Bacteria and the Archaea*. Springer-Verlag Berlin Heidelberg. https://doi.org/10.1007/978-3-642-38954-2_164.
89. Zhang H, Sekiguchi Y, Hanada S, Hugenholtz P, Kim H, Kamagata Y, Nakamura K. 2003. *Gemmatimonas aurantiaca* gen. nov., sp. nov., a Gram-negative, aerobic, polyphosphate-accumulating micro-organism, the first cultured representative of the new bacterial phylum Gemmatimonadetes phyl. nov. *Int J Syst Evol Microbiol* 53:1155–1163. <https://doi.org/10.1099/ijso.0.02520-0>.
90. DeBruyn JM, Nixon LT, Fawaz MN, Johnson AM, Radosevich M. 2011. Global biogeography and quantitative seasonal dynamics of Gemmatimonadetes in soil. *Appl Environ Microbiol* 77:6295–6300. <https://doi.org/10.1128/AEM.05005-11>.
91. Pascault N, Ranjard L, Kaisermann A, Bachar D, Christen R, Terrat S, Mathieu O, Lévêque J, Mougel C, Henault C, Lemanceau P, Péan M, Boiry S, Fontaine S, Maron P-A. 2013. Stimulation of different functional groups of bacteria by various plant residues as a driver of soil

- priming effect. *Ecosystems* 16:810–822. <https://doi.org/10.1007/s10021-013-9650-7>.
92. Castelle CJ, et al. 2013. Extraordinary phylogenetic diversity and metabolic versatility in aquifer sediment. *Nat Commun* 4:1–10.
 93. Momper L, Jungbluth SP, Lee MD, Amend JP. 2017. Energy and carbon metabolisms in a deep terrestrial subsurface fluid microbial community. *ISME J* 11:2319–2333. <https://doi.org/10.1038/ismej.2017.94>.
 94. Strous M, Pelletier E, Mangenot S, Rattei T, Lehner A, Taylor MW, Horn M, Daims H, Bartol-Mavel D, Wincker P, Barbe V, Fonknechten N, Vallenet D, Segurens B, Schenowitz-Truong C, Médigue C, Collingro A, Snel B, Dutilh BE, Op den Camp HJM, van der Drift C, Cirpus I, van de Pas-Schoonen KT, Harhangi HR, van Niftrik L, Schmid M, Keltjens J, van de Vossenberg J, Kartal B, Meier H, Frishman D, Huynen MA, Mewes H-W, Weissenbach J, Jetten MSM, Wagner M, Le Paslier D. 2006. Deciphering the evolution and metabolism of an anaerobic bacterium from a community genome. *Nature* 440:790–794. <https://doi.org/10.1038/nature04647>.
 95. Zhao R, Summers ZM, Christman GD, Yoshimura KM, Biddle JF. 2020. Metagenomic views of microbial dynamics influenced by hydrocarbon seepage in sediments of the Gulf of Mexico. *Sci Rep* 10:1–13.
 96. Dong X, Greening C, Bröls T, Conrad R, Guo K, Blaskowski S, Kaschani F, Kaiser M, Laban NA, Meckenstock RU. 2018. Fermentative Spirochaetes mediate necromass recycling in anoxic hydrocarbon-contaminated habitats. *ISME J* 12:2039–2050. <https://doi.org/10.1038/s41396-018-0148-3>.
 97. Dubinina G, Grabovich M, Leshcheva N, Rainey FA, Gavrich E. 2011. Spirochaeta perfringens sp. nov., an oxygen-tolerant, sulfide-oxidizing, sulfur- and thiosulfate-reducing spirochaete isolated from a saline spring. *Int J Syst Evol Microbiol* 61:110–117. <https://doi.org/10.1099/ijs.0.018333-0>.
 98. Delgado-Baquerizo M, Reich PB, Trivedi C, Eldridge DJ, Abades S, Alfaro FD, Bastida F, Berhe AA, Cutler NA, Gallardo A, García-Velázquez L, Hart SC, Hayes PE, He J-Z, Hseu Z-Y, Hu H-W, Kirchmair M, Neuhauser S, Pérez CA, Reed SC, Santos F, Sullivan BW, Trivedi P, Wang J-T, Weber-Grullon L, Williams MA, Singh BK. 2020. Multiple elements of soil biodiversity drive ecosystem functions across biomes. *Nat Ecol Evol* 4:210–220. <https://doi.org/10.1038/s41559-019-1084-y>.
 99. Herren CM, McMahon KD. 2018. Keystone taxa predict compositional change in microbial communities. *Environ Microbiol* 20:2207–2217. <https://doi.org/10.1111/1462-2920.14257>.
 100. Jousset A, Bienhold C, Chatzinotas A, Gallien L, Gobet A, Kurm V, Küsel K, Rillig MC, Rivett DW, Salles JF, van der Heijden MGA, Youssef NH, Zhang X, Wei Z, Hol WHG. 2017. Where less may be more: how the rare biosphere pulls ecosystems strings. *ISME J* 11:853–862. <https://doi.org/10.1038/ismej.2016.174>.
 101. Lynch MDJ, Neufeld JD. 2015. Ecology and exploration of the rare biosphere. *Nat Rev Microbiol* 13:217–229. <https://doi.org/10.1038/nrmicro3400>.
 102. Connell JH. 1978. Diversity in tropical rain forests and coral reefs. *Science* 199:1302–1310. <https://doi.org/10.1126/science.199.4335.1302>.
 103. Sommer U, Padisák J, Reynolds CS, Juhász-Nagy P. 1993. Hutchinson's heritage: the diversity-disturbance relationship in phytoplankton. *Hydrobiologia* 249:1–7. <https://doi.org/10.1007/BF00008837>.
 104. Kristensen E, Holmer M, Bussarawit N. 1991. Benthic metabolism and sulfate reduction in a Southeast Asian mangrove swamp. *Mar Ecol Prog Ser* 73:93–103. <https://doi.org/10.3354/meps073093>.
 105. Varon-Lopez M, Dias ACF, Fasanella CC, Durrer A, Melo IS, Kuramae EE, Andreote FD. 2014. Sulphur-oxidizing and sulphate-reducing communities in Brazilian mangrove sediments. *Environ Microbiol* 16:845–855. <https://doi.org/10.1111/1462-2920.12237>.
 106. Bartlett KB, Bartlett DS, Harriss RC, Sebacher DI. 1987. Methane emissions along a salt marsh salinity gradient. *Biogeochemistry* 4:183–202. <https://doi.org/10.1007/BF02187365>.
 107. Poffenbarger HJ, Needelman BA, Meganigal JP. 2011. Salinity influence on methane emissions from tidal marshes. *Wetlands* 31:831–842. <https://doi.org/10.1007/s13157-011-0197-0>.
 108. Zhang X, Hu BX, Ren H, Zhang J. 2018. Composition and functional diversity of microbial community across a mangrove-inhabited mudflat as revealed by 16S rDNA gene sequences. *Sci Total Environ* 633:518–528. <https://doi.org/10.1016/j.scitotenv.2018.03.158>.
 109. Boschker HTS, Vasquez-Cardenas D, Bolhuis H, Moerdijk-Poortvliet TWC, Moodley L. 2014. Chemoautotrophic carbon fixation rates and active bacterial communities in intertidal marine sediments. *PLoS One* 9: e101443. <https://doi.org/10.1371/journal.pone.0101443>.
 110. Louca S, Wegener Parfrey L, Doebeli M. 2016. Decoupling function and taxonomy in the global ocean microbiome. *Science* 353:1272–1277. <https://doi.org/10.1126/science.aaf4507>.
 111. Gomes NCM, Cleary DFR, Calado R, Costa R. 2011. Mangrove bacterial richness. *Commun Integr Biol* 4:419–423. <https://doi.org/10.4161/cib.15253>.
 112. Cabral L, Júnior GVL, Pereira de Sousa ST, Dias ACF, Lira Cadete L, Andreote FD, Hess M, de Oliveira VM. 2016. Anthropogenic impact on mangrove sediments triggers differential responses in the heavy metals and antibiotic resistomes of microbial communities. *Environ Pollut* 216: 460–469. <https://doi.org/10.1016/j.envpol.2016.05.078>.
 113. Takahashi S, Tomita J, Nishioka K, Hisada T, Nishijima M. 2014. Development of a prokaryotic universal primer for simultaneous analysis of Bacteria and Archaea using next-generation sequencing. *PLoS One* 9: e105592. <https://doi.org/10.1371/journal.pone.0105592>.
 114. Klindworth A, Pruesse E, Schweer T, Peplies J, Quast C, Horn M, Glöckner FO. 2013. Evaluation of general 16S ribosomal RNA gene PCR primers for classical and next-generation sequencing-based diversity studies. *Nucleic Acids Res* 41:e1. <https://doi.org/10.1093/nar/gks808>.
 115. Martin M. 2011. Cutadapt removes adapter sequences from high-throughput sequencing reads. *Embnet J* 17:10–12. <https://doi.org/10.14806/ej.17.1.200>.
 116. Callahan BJ, McMurdie PJ, Rosen MJ, Han AW, Johnson AJA, Holmes SP. 2016. DADA2: high-resolution sample inference from Illumina amplicon data. *Nat Methods* 13:581–583. <https://doi.org/10.1038/nmeth.3869>.
 117. Callahan BJ, McMurdie PJ, Holmes SP. 2017. Exact sequence variants should replace operational taxonomic units in marker-gene data analysis. *ISME J* 11:2639–2643. <https://doi.org/10.1038/ismej.2017.119>.
 118. Quast C, Pruesse E, Yilmaz P, Gerken J, Schweer T, Yarza P, Peplies J, Glöckner FO. 2013. The SILVA ribosomal RNA gene database project: improved data processing and web-based tools. *Nucleic Acids Res* 41: D590–D596. <https://doi.org/10.1093/nar/gks1219>.
 119. McMurdie PJ, Holmes S. 2013. phyloseq: an R Package for reproducible interactive analysis and graphics of microbiome census data. *PLoS One* 8:e61217. <https://doi.org/10.1371/journal.pone.0061217>.
 120. Wright ES. 2016. Using DECIPHER v2.0 to analyze big biological sequence data in R. *R J* 8:352–359. <https://doi.org/10.32614/RJ-2016-025>.
 121. Schliep KP. 2011. phangorn: phylogenetic analysis in R. *Bioinformatics* 27:592–593. <https://doi.org/10.1093/bioinformatics/btq706>.
 122. Kembel SW, Cowan PD, Helmus MR, Cornwell WK, Morlon H, Ackerly DD, Blomberg SP, Webb CO. 2010. Picante: r tools for integrating phylogenies and ecology. *Bioinformatics* 26:1463–1464. <https://doi.org/10.1093/bioinformatics/btq166>.
 123. Faust K, Raes J. 2012. Microbial interactions: from networks to models. *Nat Rev Microbiol* 10:538–550. <https://doi.org/10.1038/nrmicro2832>.
 124. Weiss S, Van Treuren W, Lozupone C, Faust K, Friedman J, Deng Y, Xia LC, Xu ZZ, Ursell L, Alm EJ, Birmingham A, Cram JA, Fuhrman JA, Raes J, Sun F, Zhou J, Knight R. 2016. Correlation detection strategies in microbial data sets vary widely in sensitivity and precision. *ISME J* 10: 1669–1681. <https://doi.org/10.1038/ismej.2015.235>.
 125. Faust K, Raes J. 2016. CoNet app: inference of biological association networks using Cytoscape [version 2; referees: 2 approved]. *F1000Res* 5: 1519–1516. <https://doi.org/10.12688/f1000research.9050.1>.
 126. Bastian M, Heymann S. 2009. Gephi: an open source software for exploring and manipulating networks.
 127. Barberán A, Bates ST, Casamayor EO, Fierer N. 2012. Using network analysis to explore co-occurrence patterns in soil microbial communities. *ISME J* 6:343–351. <https://doi.org/10.1038/ismej.2011.119>.
 128. Assenov Y, Ramírez F, Schelhorn SESE, Lengauer T, Albrecht M. 2008. Computing topological parameters of biological networks. *Bioinformatics* 24:282–284. <https://doi.org/10.1093/bioinformatics/btm554>.
 129. Van Rossum G, Drake FL. 2019. The Python language reference—Python 3.7.4 documentation. <https://docs.python.org/release/3.7.4/reference/index.html>.
 130. Core Team, T. 2016. R: a language and environment for statistical computing. R Foundation for Statistical Computing, Vienna, Austria.
 131. Oksanen J, et al. 2016. Vegan: community ecology package: R package version 2.4–3.
 132. Wickham H. 2009. ggplot2: elegant Graphics for Data Analysis. Springer.
 133. Clarke K, Gorley R. 2006. PRIMER v6: user manual/tutorial. Prim Plymouth 192.